





## **Bioelectronic devices for Astrocyte-Neuron communication**

Inês Daniela Fernandes da Ponte

Thesis submitted to the Faculty of Sciences and Technology of the University of Coimbra for the degree of Master in Biomedical Engineering with specialization in Biomedical Instrumentation

Supervisor:  
Henrique Leoner Gomes (DEEC-UC)

**Coimbra 2024**

This work was founded by FCT through the project AstroNeuroCircuit: Dispositivos Bioeletrónicos para medir a comunicação astrócito-neurónio (Ref. n.º **2022.06979.PTDC**) e pelo Instituto de Telecomunicações (IT) UIDB/EEA/50008/2020.

Esta cópia da tese é fornecida na condição de que quem a consulta reconhece que os direitos de autor são da pertença do autor da tese e que nenhuma citação ou informação obtida a partir dela pode ser publicada sem a referência apropriada.

This thesis copy has been provided on the condition that anyone who consults it understands and recognizes that its copyright belongs to its author and that no reference from the thesis or information derived from it may be published without proper acknowledgement.

## **Agradecimentos**

E com grande orgulho que chego ao fim de 5 anos de aprendizagem, feliz por este percurso cheio de alegrias e histórias, amigos que se tornaram casa.

Em primeiro lugar agradecer ao meu orientador, Professor Doutor Henrique Leonel Gomes, por todo o tempo despendido, por toda a prontidão para esclarecer as minhas dúvidas e pela partilha do seu vasto conhecimento. Não esquecendo todos os restantes professores, investigadores e colegas de laboratório, assim como ao Instituto de Telecomunicações (IT). Agradecer à Dra. Rute Félix e à Aliana Vairinhos, da Universidade do Algarve, à Catarina Bispo da Universidade de Coimbra e à Gabrielle Coelho Lelis da Brazilian Nanotechnology National Laboratory – LNNano, por toda a entajuda, disponibilidade e simpatia.

Aos meus amiguinhos que fizeram de Coimbra a 2<sup>a</sup> casa, Rita, Cris e David, obrigada por tudo o que viveram comigo e pela oportunidade de conhecer pessoas incríveis como vocês.

Aos meus amigos da terrinha, que de longe acompanharam todas as vivências e que sempre me receberam de braços abertos na volta a casa.

Agradecimento especial às minhas colegas de casas e de vida, pela partilha, amizade e longas noites de conversa, mas principalmente por serem a minha base em todas as fases de vida.

Ao meu namorado por nunca me deixar desistir de nada e por me acompanhar em todos os meus dilemas e problemas, longe ou perto, sempre com a melhor disposição.

Por fim, e mesmo assim o mais importante, à minha família. Ao meu pai por me mostrar todos os dias o que é disciplina e força de vontade, à minha mãe por ser um verdadeiro exemplo em tudo o que faz e à minha irmã por ser a melhor companheira de vida que podia pedir.

Nunca conseguirei expressar por palavras o que significam para mim. Agora, ficam as memórias e a saudade desta experiência e desta cidade que tão bem acolhe quem de novo a ela chega.



## Sumário

Esta dissertação tem como objetivo investigar e registrar sinais bioelétricos extracelulares em culturas de astrócitos, um tema que tem atraído crescente atenção na investigação em neurociência. A importância de estudar a comunicação entre astrócitos assenta na hipótese de que estas células gliais desempenham um papel crucial na regulação das interações entre neurónios e na modelação dos circuitos neuronais.

Ao contrário dos neurónios, os astrócitos não geram potenciais de ação. Em vez disso, acredita-se que comunicam com os neurónios e outros astrócitos através de oscilações bioelétricas lentas e rítmicas. Alguns estudos sugerem que estas oscilações resultam de uma atividade sincronizada dos astrócitos. No entanto, o significado funcional e os mecanismos biológicos subjacentes — tais como os canais iónicos específicos e os estímulos responsáveis por gerar estes sinais oscilatórios — permanecem inexplorados.

Com base em trabalhos anteriores realizados pelo grupo de investigação anfitrião, este trabalho utiliza métodos de registo extracelular com eléctrodos desenhados para detectar pequenas oscilações bioelétricas em culturas de astrócitos. Embora estas oscilações já tenham sido observadas, o seu papel exato continua por esclarecer. Para aprofundar a nossa compreensão da comunicação entre astrócitos, são propostas duas hipóteses principais:

Hipótese I: Os aglomerados de astrócitos sincronizam a sua atividade para produzir oscilações elétricas extracelulares distintas.

Hipótese II: Estas oscilações sincronizadas podem propagar-se por populações de células interligadas, formando uma onda elétrica.

Para testar estas hipóteses, a equipa de investigação desenhou e fabricou eléctrodos com diferentes tamanhos e geometrias, explorando como estes parâmetros influenciam a potência, duração e forma dos sinais registados. A relação entre as dimensões dos eléctrodos e as características dos sinais baseia-se na premissa de que, quando as células sincronizam a sua atividade, o tamanho do aglomerado celular pode variar. Espera-se que eléctrodos maiores captem sinais de aglomerados maiores, resultando em sinais de maior potência, enquanto eléctrodos mais pequenos detetariam sinais de menor potência, provenientes de aglomerados menores.

A tese centra-se em duas principais geometrias de elétrodos: elétrodos redondos com áreas variáveis e elétrodos com extensões circulares de diferentes larguras. Os elétrodos redondos foram utilizados para examinar como o tamanho do elétrodo afeta os sinais extracelulares, enquanto os elétrodos circulares foram desenhados para investigar a possível propagação de ondas viajantes através de redes de astrócitos.

Além de investigar a relação entre as propriedades dos elétrodos e as características dos sinais, este estudo inclui experiências que envolvem a estimulação química de culturas de astrócitos. Através da administração de diferentes fármacos, a investigação visa demonstrar a capacidade de modular a atividade bioelétrica extracelular, mostrando que compostos específicos podem iniciar ou suprimir essa atividade.

Esta tese também oferece uma visão abrangente das metodologias elétricas e dos designs de elétrodos utilizados para registrar sinais de astrócitos, contribuindo para uma compreensão mais profunda das dinâmicas bioelétricas dentro destas culturas de células gliais.



## Abstract

This thesis aims to record and investigate extracellular bioelectrical signals in populations of astrocytes, a topic that has gained increasing relevance in neuroscience research. The significance of studying astrocyte communication stems from the hypothesis that these glial cells play a crucial role in regulating neuron-to-neuron communication and in shaping and configuring neural circuits.

Unlike neurons, astrocytes do not generate rapid electrical spikes. Instead, they are believed to communicate with nearby neurons and other astrocytes through slower, rhythmic electrical oscillations. Some studies suggest that these oscillations result from synchronized activity within clusters of astrocytes. However, the functional role and underlying biological mechanisms of these signals, such as the specific ion channels and triggers responsible for generating discrete oscillatory signals, remain largely unexplored.

Building on the prior work of the hosting research group, this thesis uses previously developed methods for extracellular electrical recording using custom-designed electrodes capable of detecting small bioelectrical oscillations in astrocyte populations. While these oscillations have been recorded, their precise function is still unclear. To advance our understanding of astrocyte communication, two key hypotheses are proposed:

Hypothesis 1: Astrocyte clusters synchronize their activity to produce discrete extracellular electrical oscillations.

Hypothesis 2: The synchronized oscillations can propagate across connected cell populations in the form of an electrical wave.

To test these hypotheses, the research team designed and fabricated electrodes with varying areas and geometries, investigating how these parameters affect the power, duration, and shape of the recorded signals. The relationship between electrode dimensions and signal characteristics is grounded in the assumption that when cells synchronize their activity, the size of the participating cell cluster may vary. Larger electrodes are expected to capture signals from larger clusters, which should result in higher signal power, while smaller area electrodes would detect lower-power signals from smaller clusters. Consequently, a distribution of signal powers is anticipated, with larger-area electrodes expected to record more high-power signals compared to smaller-area electrodes.

## Abstract

---

The thesis primarily focuses on two types of electrode geometries: round electrodes of varying areas and circular electrodes with differently-sized fingers. The round electrodes were used to study how electrode size influences extracellular signals, while the fingered circular electrodes were specifically designed to investigate the presence of traveling waves across the astrocyte network.

In addition to exploring the relationship between electrode properties and signal characteristics, the research includes experiments involving chemical stimulation of astrocyte populations. By administering different drugs, the study seeks to demonstrate the ability to modulate extracellular bioelectrical activity, showing that specific compounds can either initiate or suppress this activity.

This thesis also provides an overview of the electrical methodologies and electrode designs used for recording astrocyte signals, contributing to a deeper understanding of the bioelectrical dynamics within these glial cell populations.

# Contents

List of Figures .....	xii
List of Tables .....	xv
List of Abbreviations .....	xvi
1.Introduction .....	1
1.1. Context and Motivation.....	2
1.2. Document Structure .....	3
2.State of the art.....	5
2.1. Introduction .....	6
2.2. Recording Techniques.....	6
2.2.1 Patch-clamp .....	7
2.2.2 Microelectrodes Arrays.....	8
2.2.3 Optical Methods .....	9
2.3. Summary.....	9
3. Fundamental Background.....	11
3.1. Introduction .....	12
3.2. Terminology and concepts .....	12
3.3 Summary.....	19
4. Long-term stability of the electrical double-layer impedance.....	20
4.1. Introduction .....	21
4.2. Methodology and experiments .....	27
4.2.1. Experimental setup .....	27
4.2.2. Electrodes .....	28
4.2.3- Culture Media .....	28
4.2.4 Experience Description .....	29
4.3. Results.....	29
4.3.1. Design Rules .....	29
4.3.2. Media Results.....	32
4.4. Discussion .....	34
4.5. Conclusions.....	36
5. Extracellular Astrocyte Signals: The role of the electrode geometry on the signal duration .....	37
5.1. Introduction .....	38
5.2. Methods.....	39

# Contents

---

5.3.	Results.....	41
5.3.1	Electrophysiological time traces .....	41
5.4.	Signal analysis .....	42
5.5.	Dependence of the signal duration on the area and geometry of the electrode .....	43
5.6.	Discussion and Conclusions .....	47
6.	Chemical Stimulation of Astrocytes .....	48
6.1.	Introduction .....	49
6.2.	Drug description .....	49
6.3.	Experimental Methods .....	53
6.4	Results and analysis .....	54
6.4.	Discussion .....	66
6.5.	Conclusions .....	67
7.	Conclusions and future work .....	69
7.1.	Main topics studied .....	70
7.2.	Conclusions .....	70
7.3.	Further work .....	72
	Bibliography .....	74

## List of Figures

<b>Figure 3. 1</b> Astrocytes and their interaction with neurons. (a) Schematic representation of astrocytes in a neural network comprised of neurons. (b) Schematic representation of how a single astrocyte may modulate several synapses. (c) Fluorescence image showing a single astrocyte and the surrounding synapses (in green), from <a href="https://neurosciencenews.com/astrocytes-neural-connections-7899/">https://neurosciencenews.com/astrocytes-neural-connections-7899/</a> . (d) Photograph of a culture of astrocytes on top of a glass (obtained in our laboratory). .....	13
<b>Figure 3.2</b> Schematic diagram of a Tripartite synapse.....	16
<b>Figure 3. 3</b> Membrane Equivalent Circuit .....	19
<b>Figure 4. 1</b> Illustration of the electrical coupling of extracellular signals detected with microelectrodes. ....	23
<b>Figure 4. 2</b> Randles and Somerton electrode-electrolyte model.....	24
<b>Figure 4. 3</b> (a) Double RC circuit used to describe electrodes immersed into an electrolyte system (b) Equivalent Circuit assumed by the impedance analyzer. The impedance analyser measures $C_p$ and $R_p$ , which are related to the equivalent circuit that describes the system. ....	25
<b>Figure 4. 4</b> Acquisition signals system illustration.....	27
<b>Figure 4. 5</b> Acquisition signals system components: Voltage preamplifier; Digital Signal Analyser; Computer using application for signal analysis.....	27
<b>Figure 4. 6</b> Equivalent circuit (Fig. 4.3a) frequency response.....	30
<b>Figure 4. 7</b> Frequency response with multiple values for the $C_D$ component: $C_D = 3\text{nF}$ (initial), $C_D = 4.5\text{nF}$ , $C_D = 6\text{nF}$ (see circuit in Fig. 4.3a).....	30
<b>Figure 4. 8</b> EDL frequency response with multiple values for the $R_D$ component: $R_D = 3\text{M}\Omega$ (initial), $R_D = 4.5\text{M}\Omega$ , $R_D = 6\text{M}\Omega$ , $R_D = 8\text{M}\Omega$ .....	31
<b>Figure 4. 9</b> EDL frequency response with multiple values for the $C_E$ component: $C_E = 0.5\text{nF}$ (initial), $C_E = 2\text{nF}$ , $C_E = 3.5\text{nF}$ , $C_E = 5\text{nF}$ .....	31
<b>Figure 4. 10</b> EDL frequency response with multiple values for the $R_E$ component: $R_E = 30\text{k}\Omega$ (initial), $R_E = 60\text{k}\Omega$ , $R_E = 90\text{k}\Omega$ , $R_E = 120\text{k}\Omega$ .....	32
<b>Figure 4. 11</b> Comparison of the capacitance and loss at the beginning ( $t=0\text{h}$ ) ( $C_i$ and $L_i$ ) and at the end ( $t=42.7\text{h}$ ) ( $C_f$ and $L_f$ ) of the experiment with DMEM media. ....	32
<b>Figure 4. 12</b> Comparison of the capacitance and loss at the beginning ( $t=0\text{h}$ ) ( $C_i$ and $L_i$ ) and at the end ( $t=43.4\text{h}$ ) ( $C_f$ and $L_f$ ) of the experiment with F-12K media.....	33
<b>Figure 4. 13</b> Comparison of the capacitance and loss at the beginning ( $t=0\text{h}$ ) ( $C_i$ and $L_i$ ) and at the end ( $t=45.4\text{h}$ ) ( $C_f$ and $L_f$ ) of the experiment with media containing KCl 10mM and Fructose 20%. ....	33
<b>Figure 4. 14</b> Comparison of the capacitance and loss at the beginning ( $t=0\text{h}$ ) ( $C_i$ and $L_i$ ) and at the end ( $t=33.6\text{h}$ ) ( $C_f$ and $L_f$ ) of the experiment with media containing KCl 6mM and Fructose 20%. ....	34
<b>Figure 4. 15</b> Comparison of the capacitance and loss at the beginning ( $t=0\text{h}$ ) ( $C_i$ and $L_i$ ) and at the end ( $t=34.2\text{h}$ ) ( $C_f$ and $L_f$ ) of the experiment with media containing KCl 16mM.....	34
<b>Figure 5. 1</b> Conceptual view of recording a travelling wave using extracellular electrodes. (a) wave crossing an electrode with width $W_1$ . (b) A wave crossing a shorter electrode with width $W_2$ . ....	38
<b>Figure 5.2</b> Patterns of circular concentric rings with different widths. (a) schematic diagram with the dimensions. (b) Gold electrode fabricated in a glass substrate. (c) electrode pattern	

## List of Figures

---

fabricated on a thermally oxidized silicon wafer. (d) A photograph of the central region clearly shows the electrodes. ....	40
<b>Figure 5. 3</b> (a) Commercially available electrodes from applied Biophysics (ref. 8W1E PET) device with 8 wells. (b) Schematic representation of the electrode geometry. ....	41
<b>Figure 5. 4</b> Electrical signals captured from a population of astrocytes, an overview of a long-term experiment. ....	42
<b>Figure 5. 5</b> Typical shapes of biphasic signals recorded in astrocyte populations. The duration $\Delta t$ of the short signal component was used as a quantification parameter to define the signal duration. ....	42
<b>Figure 5. 6</b> Typical biphasic signals in an astrocyte population. ....	43
<b>Figure 5. 7</b> Comparison of signal duration for circular electrodes with different electrode widths. Electrode geometry is represented in Figure 5.2. $d$ being the width of the electrode..	45
<b>Figure 5. 8</b> Comparison of signal duration for round electrodes with different electrode areas. Electrode geometry is represented in Figure 5.3. ....	46
<b>Figure 6. 1</b> (a) Recordings of bioelectrical activity before, during and after administration of EGTA at a concentration of 100 $\mu\text{M}$ (b) Power spectral density of the voltage noise, $S_V$ , as a function of frequency.(A) Before exposure (B) During exposure and (C) Drug wash with replacement with a fresh cell-culture medium. ....	55
<b>Figure 6. 2</b> (a) Recordings of bioelectrical activity before, during and after administration of EGTA at a concentration of 500 $\mu\text{M}$ (b) Power spectral density of the voltage noise, $S_V$ , as a function of frequency.(C) Before exposure (D) During exposure and (E) Drug wash with replacement with a fresh cell-culture medium. ....	56
<b>Figure 6. 3</b> Bioelectrical response of an astrocyte population to two consecutive EGTA administrations at increasing concentrations. ....	57
<b>Figure 6. 4</b> (a) Recordings of bioelectrical activity before, during and after administration of caffeine at a concentration of 2.5 mM (b) Power spectral density of the voltage noise, $S_V$ , as a function of frequency.(A) Before exposure (B) During exposure and (C) Drug wash with replacement with a fresh cell-culture medium. ....	58
<b>Figure 6. 5</b> (a) Recordings of astrocyte bioelectrical activity before, during and after administration of $\text{CaCl}_2$ at a concentration of 5 mM (b) Power spectral density of the voltage noise, $S_V$ , as a function of frequency. (A) Before exposure (B) During exposure and (C) Drug wash with replacement with a fresh cell-culture medium. ....	59
<b>Figure 6. 6</b> (a) Recordings of bioelectrical activity before, during and after administration of $\text{CaCl}_2$ at a concentration of 10 mM (b) Power spectral density of the voltage noise, $S_V$ , as a function of frequency. (A) Before exposure (B) During exposure and (C) Drug wash with replacement with a fresh cell-culture medium. ....	59
<b>Figure 6. 7</b> The effect of $\text{CaCl}_2$ administration on the astrocyte activity. Two consecutive administrations with increasing $\text{CaCl}_2$ concentrations were carried out. ....	60
<b>Figure 6. 8</b> (a) Recordings of bioelectrical activity before, during and after administration of norepinephrine at a concentration of 5 mM (b) Power spectral density of the voltage noise, $S_V$ , as a function of frequency. (A) Before exposure (B) During exposure and (C) Drug wash with replacement with a fresh cell-culture medium. ....	60
<b>Figure 6. 9</b> (a) Recordings of bioelectrical activity before, during and after administration of dopamine at a concentration of 10 mM (b) Power spectral density of the voltage noise, $S_V$ , as a function of frequency. (A) Before exposure (B) During exposure and (C) Drug wash with replacement with a fresh cell-culture medium. ....	61
<b>Figure 6. 10</b> (a) Recordings of bioelectrical activity before, during and after administration of dopamine at a concentration of 2.5 mM (b) Power spectral density of the voltage noise, $S_V$ , as a	

## List of Figures

---

function of frequency. (A) Before exposure (B) During exposure and (C) Drug wash with replacement with a fresh cell-culture medium .....	62
<b>Figure 6. 11</b> The astrocyte bioelectrical activity response to two consecutive dopamine exposures with increasing concentration.....	62
<b>Figure 6. 12 (a)</b> Recordings of bioelectrical activity before, during and after administration of glutamate at a concentration of 2.5 mM <b>(b)</b> Power spectral density of the voltage noise, $S_V$ , as a function of frequency. (A) Before exposure (B) During exposure and (C) Drug wash with replacement with a fresh cell-culture medium. ....	63
<b>Figure 6. 13 (a)</b> Recordings of bioelectrical activity before, during and after administration of glutamate at a concentration of 5 mM <b>(b)</b> Power spectral density of the voltage noise, $S_V$ , as a function of frequency. (A) Before exposure (B) During exposure and (C) Drug wash with replacement with a fresh cell-culture medium .....	64
<b>Figure 6. 14</b> The astrocyte response to two consecutive glutamate exposures with increasing concentration. ....	64
<b>Figure 6. 15 (a)</b> Recordings of bioelectrical activity before, during and after acidic medium administration (pH=6.2) <b>(b)</b> Power spectral density of the voltage noise, $S_V$ , as a function of frequency. (A) Before exposure (B) During exposure and (C) Drug wash with replacement with a fresh cell-culture medium.....	65
<b>Figure 6. 16 (a)</b> Recordings of bioelectrical activity before, during and after acidic medium administration (pH=5.4) <b>(b)</b> Power spectral density of the voltage noise, $S_V$ , as a function of frequency.(C) Before exposure (D) During exposure and (E) Drug wash with replacement with a fresh cell-culture medium.....	65
<b>Figure 6. 17</b> The response of astrocytes to two consecutive pH changes.....	66

## List of Tables

<b>Table 4. 1</b> Time influence on the values of each component .....	35
<b>Table 6. 1</b> Drugs used in this study. The concentration and exposure times are outlined.....	54
<b>Table 6. 2</b> Main conclusions of each drug.....	67



## List of Abbreviations

<b>AP</b>	Action Potential
<b>MEAs</b>	Microelectrode Arrays
<b>CNS</b>	Central Nervous System
<b>SNR</b>	Signal-to-noise Ratio
<b>AC</b>	Alternative Current
<b>PET</b>	Polyethylene terephthalate
<b>DMEM</b>	Dulbecco's Modified Eagle Medium
<b>F12-K</b>	Kaighn's Modification of Ham's F-12 Medium
<b>EGTA</b>	Ethylene glycol-bis( $\beta$ -aminoethyl ether)-N,N,N',N'-tetraacetic acid
<b>pHi</b>	Intracellular pH

# **Chapter 1**

## **Introduction**

This introductory chapter offers an overview of the research conducted in this thesis, outlining the motivation, key objectives, and scientific significance. Additionally, it summarises the document's structure and briefly describes the content of the following chapters.

# 1. Introduction

---

## 1.1. Context and Motivation

The study of bioelectricity began in 1780 when Luigi Galvani conducted pioneering experiments demonstrating electrical interactions in living tissues [1]. His work inspired the scientific community to extensively explore electrical phenomena in biological cells and tissues. Decades later, advancements by Hodgkin and Huxley in neurophysiology [2]—particularly in understanding nerve conduction and excitation—were crucial in defining the concept of electrogenic cells capable of generating action potentials (APs) [3]. With the development of techniques such as patch-clamp, microelectrodes, and microelectrode arrays (MEAs), it became possible to record the electrical activity of these cells with high precision.

However, beyond the electrical activity of neurons, there exists a bioelectrical communication in non-electrogenic cells that plays a vital role in the biology of multicellular organisms. Non-electrogenic cells, do not generate APs, instead they use ionic flows and voltage gradients to communicate and coordinate essential biological functions such as cell migration, tissue repair, and proliferation. The bioelectrical signals generated by these cells occur over much longer time scales and have amplitudes often in the microvolt range.

Electrical techniques are not selective. This means that they cannot identify the specific ionic species responsible for the ionic fluctuations, but they have the advantage of being entirely non-invasive and capable of monitoring bioelectrical fluctuations over extended periods, ranging from several hours to several weeks, in real-time. Therefore, extracellular electrodes and electrical techniques are highly valuable for tracking changes in cellular activity over time and for studying the dynamics of cell-cell communication.

Detecting and recording these subtle signals presents a significant challenge, as traditional electrophysiological methods were not designed to capture such minimal variations. Therefore, there is a growing demand for specialized devices capable of monitoring the bioelectrical activity of non-electrogenic cells in real time.

The cells studied in this project are astrocytes, glial cell which were once thought to be passive, space-filling components of the nervous system. However, recent research has increasingly highlighted their pivotal role in regulating synaptic transmission, synapse formation, and neural plasticity.

This study aims to use extracellular electrodes capable of recording electrical fluctuations in populations of astrocytes, with a particular focus on how electrode parameters

# 1. Introduction

---

influence the quality and properties of the signals recorded. Additionally, the research assesses the ability of these recordings to capture changes in astrocyte activity induced by pharmacological agents.

This study on the role of electrodes in controlling the quality of bioelectrical recordings is highly significant, as it will provide crucial insights for designing electrodes with optimised geometries and sensing areas, ultimately enhancing the signal-to-noise ratio (SNR) of bioelectrical signals. On a fundamental level, our findings may provide insight into on how astrocytes communicate with each other and with neurons. The knowledge gained could pave the way for novel therapeutic approaches targeting neurodegenerative diseases, particularly those that rely on the use of electric fields.

## 1.2. Document Structure

The structure of this document is organized into seven chapters. Following this introduction, the subsequent chapters are arranged as follows:

Chapter 2, entitled State of the Art, reviews the tools and methodologies used to study bioelectrical signalling. It provides an overview of how various research groups tackle the challenges of measuring cellular communication, particularly on non-electrogenic cells. The chapter evaluates the strengths and limitations of existing technologies, highlighting the need for further advancements to deepen our understanding of cellular interactions.

Chapter 3, Fundamental Background, lays the conceptual groundwork by introducing the key scientific principles and terminology essential for the discussions that follow. It opens with a concise overview of astrocytes, the primary cell type under investigation, and their functional interactions with neurons. Core concepts such as bioelectricity, electrogenic cells, and endogenous fields are introduced, providing a foundation for the more detailed analyses in the subsequent chapters.

Chapter 4 presents the methodology used for extracellular measurements. It also focuses on understanding the electrical double layer (EDL) behaviour at the electrode-cell culture medium interface. Moreover, the chapter explores the long-term stability of the EDL during extended electrophysiological measurements and investigates how the electrolyte composition influences the overall impedance of the system electrode/electrolyte.

# 1. Introduction

---

Chapter 5 examines the bioelectrical activity generated by astrocyte populations, particularly regarding the influence of electrode geometry and area on signal properties. By investigating whether the observed electrical oscillations are traveling waves or localized activities, it aims to provide a clearer understanding of the underlying patterns in astrocyte-generated signals.

Chapter 6 explores the impact of pharmacological agents on astrocyte bioelectrical activity. The primary objective was to confirm that the recorded signals were indeed generated by astrocytes' activity and to demonstrate that their activity could be effectively modulated by drug administration. These experiments act as a validation tool confirming that the signals are indeed generated by the astrocyte population.

By monitoring the bioelectrical responses both before and after the drug administration, the study revealed distinct changes in astrocyte behaviour, providing clear evidence of the cells' responsiveness to pharmacological stimuli.

The final chapter 7 synthesizes the key findings from across the thesis, drawing connections between the different experimental outcomes. It reflects on unresolved questions that emerged during the research and proposes directions for future experiments that could further elucidate some of the unsolved issues.

# **Chapter 2**

## **State of the art**

This chapter explores the various tools and techniques used to record electrical communication in glial cells, highlighting the distinct scientific communities and their approaches within this research field. The discussion reviews the strengths and limitations of current methods, emphasizing the need for technologies to become more efficient in investigating cell-to-cell communication, particularly in non-electrogenic cells.

## 2. State of the art

---

### 2.1. Introduction

For over a century, glial cells have been regarded as merely passive glue that connects and supports neurons. However, in recent years, they have been found to have diverse roles within the central nervous system (CNS). Astrocytes, the most abundant cell type in the human CNS, are considered to be directly involved in brain signaling via astrocyte–neuron interaction at tripartite synapse [4,5]. Recently, it has been proposed that astrocytes contribute to the progression of various neurodegenerative disorders such as Alzheimer’s, Parkinson’s, and Alexander’s disease [6].

The role of astrocytes has drawn significant attention from two scientific groups: biologists and the neuromorphic community. Each group approaches the topic with a distinct perspective.

Biologists primarily explore the molecular interactions between astrocytes and neurons at the synaptic level, focusing on the local exchange of biochemical signals [7,8]. The neuromorphic community uses this biological knowledge to design hardware systems that replicate brain-like functionality, with growing interest in incorporating astrocytic functions into neural networks. This community recognised the value of incorporating a second cell type to regulate signal flow across synapses and astrocytes have recently been integrated into artificial circuit designs [9].

On the other hand, once astrocytes are capable of coordinating numerous synapses simultaneously, leading to the hypothesis that they may employ more complex, large-scale communication mechanisms—potentially electrical in nature—since simple molecular signalling seems insufficient for this task. This has sparked interest within the bioelectronics community, suggesting that an electrical network operating at millihertz frequencies could enable widespread synchronization, providing an intriguing path for further exploration.

While several well-established bioelectronic methodologies exist, few have been specifically applied to astrocytes. This project aims to identify the most suitable methods for recording the extracellular signals produced by astrocytes.

### 2.2. Recording Techniques

The available methodologies for the recording of brain activity include: (a) intracellular recordings by patch-clamp electrodes (b) extracellular recordings by substrate-

## 2. State of the art

---

integrated MEAs, (c) optical imaging and stimulation technologies of extrinsic fluorescent indicators and (d) other methods such as functional magnetic resonance imaging and electroencephalography which record activity from large-scale neural populations but will not be considered, as they are not relevant to the focus of our project [10].

The patch-clamp technique is specifically designed to analyse single cells, focusing on the activity of individual ion channels in the cell membrane. Although it offers detailed information about these channels' function, the method is invasive and doesn't provide insight into how cells communicate with each other.

Optical imaging using extrinsic fluorescent indicators is a non-invasive method to monitor brain activity. It uses optical probes that emit signals when they contact specific substances. This technique allows visualization of the dynamic processes of cells. However, it requires advanced microscopes equipped with lasers and fast optical detection systems for accurate measurement.

The use of extracellular electrodes is most suitable for studying intercellular communication, since this methodology detects electrical signals generated by ion movements across cell membranes. This approach allows the study of multiple cells and their interactions within a network.

### 2.2.1 Patch-clamp

Patch clamp is a widely used technique. The method is essential for studying ionic currents in living cells. Applied in various areas such as neuroscience and electrophysiology, the literature already presents several studies focused on astrocytes [11-13].

This technique uses a glass pipette with a very fine tip. The pipette is placed on the cell membrane, creating a strong seal that blocks the flow of current between the cell and the surrounding solution. This makes it easier to control the membrane potential and the ionic environment on both sides, allowing for the measurement of electrical signals from individual channels.

Patch-clamp can be used in two main modes: voltage-clamp and current-clamp. The choice between these modes depends on the parameters being measured. Voltage-clamp is used to monitor and trigger APs, allowing precise control of the membrane potential to study specific ionic currents. Current-clamp, on the other hand, is used to measure the membrane potential or synaptic inputs [14].



## 2. State of the art

---

The patch clamp technique offers various configurations, each tailored to specific experimental objectives. In the cell-attached configuration, the pipette is sealed to the cell membrane without breaking it, allowing the study of ion channel activity while preserving the intracellular contents. The whole-cell technique involves rupturing the membrane to access the cell's interior, making it ideal for studying electrical currents across the entire cell. In the inside-out configuration, a fragment of the membrane is removed, enabling the analysis of ion channels on the intracellular side. In the outside-out mode, after the pipette is retracted, the membrane reorganizes, allowing the study of interactions between the membrane and the extracellular environment [15].

### 2.2.2 Microelectrodes Arrays

MEAs are devices used to record the electrical activity of neural networks *in vitro*, offering a non-invasive approach that preserves the natural state of cells during measurements. These arrays consist of a grid of small electrodes fabricated on a substrate, designed to detect extracellular signals generated by the movement of ions across cell membranes during cell activity

MEAs function by detecting the potential difference between the electrodes and the extracellular environment. Their spatial resolution depends on the number of electrodes and their spacing, while their temporal resolution is determined by their ability to quickly capture and process rapid variations in electrical potentials [10,16]. (This high detection capacity makes them particularly valuable in studies involving cellular communication and intercellular signaling.)

A recent study involving the use of implanted MEAs in the brain revealed that the inherent mechanical and chemical mismatch between brain tissue and MEAs leads to several undesirable effects. For instance, MEA micromotion not only causes damage and alterations to the brain but also compromises the functionality of the MEAs [17].

In general, there are few studies reporting astrocyte activity using MEAs. However, it has been demonstrated that spike trains and glial responses can be simultaneously captured from individual sensing electrodes [18]. Additionally, it has been proven that astrocytes can be electrically stimulated and exhibit extracellular voltage fluctuations across a broad frequency spectrum when using MEAs [19].

Primary cultures were used to measure spontaneous electrophysiological activity in astrocytes [20,21] and record high-frequency voltage oscillations caused by electrical

## 2. State of the art

---

stimulation of astrocytic cells. Ultra-weak signals and noisy electrical fluctuations generated by populations of glioma cells were also reported [22]. The strategy enabling the observation of these weak signals exploits large capacitive electrodes with a low intrinsic thermal noise.

### 2.2.3 Optical Methods

In parallel with the development of extracellular MEAs, efforts have been made to advance optical imaging approaches. These methods include imaging membrane potentials with voltage-sensitive dyes, monitoring changes in intracellular calcium concentrations, and tracking intrinsic signals.

MEAs have recently been combined with optical techniques like calcium fluorescence imaging. The combination of these two approaches has provided deeper insights into the relationship between electrical activity and intracellular calcium signals. By synchronizing the recording of electrophysiological data with calcium imaging, researchers have shown that astrocytes respond to electrical stimulation by generating membrane voltage oscillations (small membrane potential deflections) along with simultaneous calcium wave production [23].

Fluorescence studies, particularly calcium imaging, have greatly advanced our understanding of astrocytes, revealing their crucial role in synaptic regulation [24,25].

Despite their advantages, optical imaging techniques face notable limitations, including the need to incubate the cells with fluorescent molecules, which have a lifespan of only a few hours. Furthermore, which molecular targets should be prioritized to study extracellular astrocyte signalling remains unclear. Additionally, exposing cells to light pulses may interfere with their normal behaviour.

In fact, recent advances in optical fluorescence methods have focused on increasing detection speed, which runs counter to the goals of our project [26].

### 2.3. Summary

Among the various methodologies for measuring brain signals and neural networks, MEAs are the most suitable. Patch-clamp techniques, while useful for individual cells, cannot capture the dynamics of cellular communication within a network. However, MEAs and their associated systems are primarily optimized for detecting APs. In contrast, the ionic fluctuations generated by astrocytes are approximately a thousand times weaker

## 2. State of the art

---

and significantly slower, lasting several seconds to minutes, with amplitudes of only a few microvolts.

This chapter highlights the need for developing novel specialized MEAs to capture these ultra-low frequency signals. When measuring non-electrogenic cells, the instrumentation must be highly sensitive to low frequencies, with devices that feature exceptionally low noise levels to ensure a high SNR.

# **Chapter 3**

## **Fundamental Background**

This chapter establishes the foundational concepts and terminology used in the subsequent chapters. It begins with a brief explanation of astrocytes, the primary cell type examined in this study, and their interactions with neurons. A concise introduction to how bioelectricity is generated by different types of cells is provided. Key terms such as electrogenic cells, endogenous fields, and APs are explained within the context of this thesis.

## 3. Fundamental Background

---

### 3.1. Introduction

This thesis is a study at the intersection between biology and electronics. Throughout this document, various terms and concepts are introduced, which may be more or less familiar depending on the reader's background. To facilitate understanding, this chapter provides a brief glossary of key concepts that will be later mentioned.

### 3.2. Terminology and concepts

#### **Electrogenic cells and non-electrogenic cells**

Biologists classify cells into two categories: electrogenic and non-electrogenic cells. Electrogenic cells are those capable of generating electrical impulses, such as APs or cardiac impulse. Examples of electrogenic cells include neurons, cardiac cells, and nerve cells. In contrast, non-electrogenic cells, such as skin cells, lung cells, and others, do not produce individual electrical spikes [27]. Despite being classified as non-electrogenic, most cells possess a complex machinery of pumps, transporters, and ion channels that enable the cells to exchange ions with the extracellular environment.

Although non-electrogenic cells do not generate spikes, they can produce voltage fluctuations in the surrounding medium. These charges generate electric fields known as endogenous fields. It is also known that they often coordinate these ionic exchanges to generate electrical oscillations or waves that can propagate through biological tissue. These oscillations are very different from an AP because they travel very slowly when compared with the speed of an AP. The electrical fluctuation of the AP travels at the speed of meters per second, a calcium wave for instance, travels at a speed of tens of micrometers per second. The speed of calcium is one million times slower than the travel speed of an AP. The major object of this thesis is the cell called the astrocyte. The astrocyte is a neural cell that is classified as non-electrogenic.

#### **Astrocytes**

Astrocytes have a star-like shape with multiple branches connecting synapses between neurons. A single astrocyte can interact with thousands of synapses allowing it to influence many neurons simultaneously. Additionally, astrocytes can form connections

### 3. Fundamental Background

with neighbouring astrocytes through gap junctions, creating a network that uses calcium to communicate (see Fig. 3.1). Astrocytes also have sodium and potassium channels that create ionic currents, but unlike neurons, they do not generate or propagate AP. However, astrocytes are considered “excitable” because, when activated by internal or external signals, they deliver specific messages to neighbouring cells.

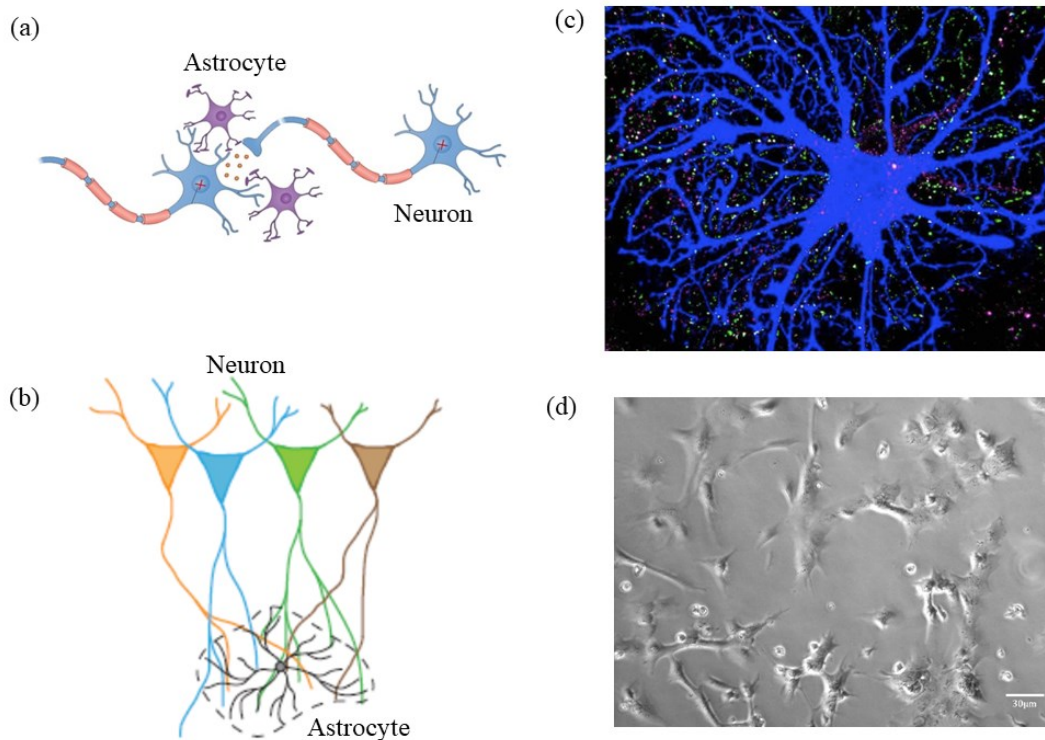


**Figure 3. 1** Astrocytes and their interaction with neurons. (a) Schematic representation of astrocytes in a neural network comprised of neurons. (b) Schematic representation of how a single astrocyte may modulate several synapses. (c) Fluorescence image showing a single astrocyte and the surrounding synapses (in green), from <https://neurosciencenews.com/astrocytes-neural-connections-7899/> . (d) Photograph of a culture of astrocytes on top of a glass (obtained in our laboratory).

Astrocytes are proposed to be involved in the pathogenesis of numerous motor disorders, including Parkinson’s disease [28-30], amyotrophic lateral sclerosis [31,32], and Tourette’s Syndrome [33,34].

#### Neurons

### 3. Fundamental Background

---

The 80 to 100 billion neurons are fundamental cells of the nervous system, responsible for transmitting information through electrochemical signals. Structurally, neurons consist of a cell body, dendrites, and an axon. Dendrites receive signals from other neurons, while the axon transmits these signals to other neurons or effector cells [35].

The significance of neurons lies in their ability to form complex communication networks that enable all brain functions, from regulating basic processes like breathing to higher cognitive functions such as memory and reasoning.

Unlike astrocytes, neurons are considered electrogenic cells, a term associated with their ability to generate APs, that are just a few milliseconds long and are commonly referred to as spikes. In comparison, the ionic fluctuations generated by astrocytes are approximately one thousand times weaker and slower.

For many years, neurons have been the focus of the electrophysiological scientific community, with attention directed towards recording APs using techniques like voltage clamp, patch-clamp, sharp electrodes and microwires.

#### **Endogenous Fields**

Endogenous electric fields (EFs) are generated by the movement of ions and charged biomolecules across cell membranes, creating voltage gradients between cells. These gradients are not only formed by small ions like protons, sodium, and potassium, but also by larger molecules such as tissue factors, growth hormones, neurotransmitters, and signaling molecules [36].

At cellular level, EFs directly influence cell orientation, migration, adhesion, proliferation, and differentiation. By depolarizing or hyperpolarizing membrane potentials, EFs can trigger the expression of signaling factors that modulate processes like cellular regeneration and tissue remodeling. This electrophysiological interaction impacts gene expression and, consequently, cell morphology, becoming part of a complex biological control system [37].

During embryonic development, EFs help establish voltage gradients that guide the formation of body axes, providing spatial orientation for the organism's development and in wound healing processes, endogenous EFs are amplified in response to epithelial injuries, directing the migration of epithelial cells toward the wound site, promoting tissue regeneration. EFs also regulate the extent and the direction of nerve growth [38].

### 3. Fundamental Background

---

#### Synapse

Synapses are the junctions between two neurons and involve the release of neurotransmitters from a presynaptic neuron into the synaptic space. These neurotransmitters bind to receptors on the postsynaptic neuron, generating an AP [39].

When an AP reaches the axon terminal of a presynaptic neuron, voltage-gated calcium channels open, allowing calcium ions to enter the terminal. This triggers the fusion of neurotransmitter-filled vesicles with the neuron's plasma membrane, releasing them into the synaptic cleft. The neurotransmitters cross this cleft and bind to specific receptors on the postsynaptic neuron's membrane [40].

After the neurotransmitters are released and act on the receptors, they can be either reabsorbed by the presynaptic neuron for reuse or degraded by enzymes in the synaptic cleft. This process ensures that signals are discrete and prevents continuous stimulation of the postsynaptic receptors. The balance between synaptic excitation and inhibition is crucial for the proper functioning of the nervous system.

#### Tripartite synapse

Astrocytes play an important role in regulating neuronal excitability, and several authors even propose that astrocytes should be regarded as integral modulatory elements of synapses [41,42]. In this context, the concept of the tripartite synapse has emerged. This concept suggests that astrocytic processes, which surround both pre- and postsynaptic areas, can respond to neurotransmitters released by neurons and also release substances called gliotransmitters, which influence neuronal activity [43]. It is important to note that astrocytes don't cover all synapses. Still, in the hippocampus, 60-90% of synapses are covered by astrocytic processes, and changes in the structure of these astrocytes can significantly impact synaptic function. Besides locally controlling synaptic functions, astrocytes form networks called astrocytic syncytia, in which neuronal circuits are embedded [44]. These networks help slowly integrate information from thousands of synapses, adjusting the overall functioning of neuronal circuits. This network organization allows astrocytes to communicate through specialized pathways.



### 3. Fundamental Background

---

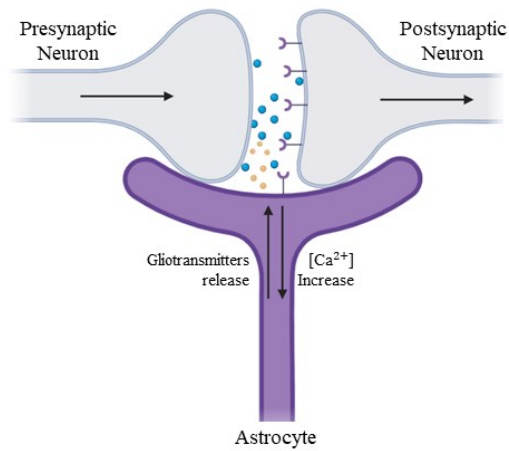


**Figure 3.2** Schematic diagram of a Tripartite synapse

#### Gap junctions

Gap junction channels connect the cytoplasm of adjacent cells, allowing for rapid exchange of ions and small molecules between adjacent cells. These channels are formed by connexins, a family of homologous proteins specialized in creating intercellular channels that enable extensive electrical and metabolic coupling between cells. Astrocytes, in particular, express high levels of connexins [45]. This connectivity is integral to the energy supply to neurons, buffering extracellular  $K^+$  and glutamate, and propagating calcium waves.

The modulation of gap junction coupling by various neuroactive substances suggests that these channels can dynamically open and close in response to neuronal activity [46]. Furthermore, the conductance of gap junctions is influenced by voltage, meaning the passage of ions through these channels varies with the electrical potential difference between connected cells [47]. Local blockade of gap junctions reduces the magnitude of membrane voltage oscillations.

#### Cell-Cell communication

Cell communication mechanisms are essential for the proper functioning of multicellular organisms and can be classified into (a) chemical, (b) electrical, and (c) physical communication.

### 3. Fundamental Background

---

Electrical communication involves signal transmission through chemical and electrical synapses. In chemical synapses, neurotransmitters are released by the presynaptic cell and bind to receptors on the postsynaptic cell, triggering a rapid response. Electrical synapses, on the other hand, allow direct ion passage through gap junctions, facilitating quick and efficient synchronization of neuronal activity. This mechanism is crucial during nervous system development and in rapid responses to stimuli [48].

Physical communication between cells is mediated mainly by gap junctions, which are channels that enable the direct transfer of small molecules and ions between adjacent cells. These channels are formed by proteins called connexins and play a vital role in coordinating cellular responses in tissues, allowing groups of cells to respond synchronously to external signals.

Chemical communication includes autocrine, paracrine, and endocrine signalling. Autocrine signals are released by a cell and act on receptors on the same cell, regulating processes like cell differentiation and inflammatory responses. Paracrine signalling occurs between nearby cells, where signals are quickly degraded or absorbed to maintain a localized response. Endocrine signalling involves hormones that travel through the bloodstream to distant target cells, producing slower but long-lasting responses.

#### **Calcium Waves**

Astrocytes are now recognized for their unique excitability characterized by intricate calcium signalling and the propagation of calcium waves.

These glial cells have the ability to propagate increases in intracellular calcium concentrations  $[Ca^{2+}]$  from a single cell to neighbouring cells, forming a wave-like pattern of communication. This calcium signalling can occur spontaneously or in response to various external stimuli. The cellular sources of astrocyte  $Ca^{2+}$  signals include multiple pathways, including those involving various receptors, channels, exchangers and pumps on the plasma membrane, as well as within intracellular organelles such as mitochondria, endoplasmic reticulum, Golgi and acidic organelles [49].

Weak and slow bioelectrical signals in astrocytes are generated by shifts in membrane potential, resulting from the movement of charged ions into or out of the cells, closely linked to calcium waves, although astrocytes possess a variety of ion channels that can also influence changes in membrane potential, for example,  $Na^+$  [21].

### 3. Fundamental Background

---

#### Cell Structure

Eukaryotic cells, including glial and neuronal cells, are enclosed by a highly specialized phospholipid bilayer known as the cell membrane. This membrane and its associated transport mechanisms enable cells to generate electrical or ionic potential gradients. As a result, the origin of extracellular signals is inherently tied to the structure and function of the cell membrane. Extensive research has been devoted to understanding its diverse properties, critical for maintaining cellular integrity and regulating molecular transport.

Beyond acting as a physical boundary, the cell membrane plays a vital role in controlling the movement of molecules into and out of the cell. The phospholipid bilayer is dynamic, fluid, and selectively permeable, with its fluidity allowing proteins and lipids to move laterally within the membrane. This lateral mobility supports the membrane's ability to adapt to the changing needs of the cell [50].

#### Bioelectricity and ion channels

Today, bioelectricity is a term associated with electrogenic cells. However, in the early days, bioelectricity was discovered in the so-called non-electrogenic cells in reality in a skin wound. In 1843, Emil du Bois-Reymond built a galvanometer [51]. His device revealed that leaking out of a cut in his finger, alongside the blood, was about one micro-ampere of electrical current.

His experiment revealed that all cells could generate electrical activity. This phenomenon arises because all cells, due to the selectively permeable properties of their membranes and complex transport mechanisms, can maintain different ionic concentrations on either side of the membrane. Since ions are electrically charged particles, their movement or exchange between these two media creates a potential difference.

Bioelectronic devices can monitor and regulate the interior environment of biological objects in real-time, making them ideal for therapeutic and implantable biomedical applications, including drug delivery, electrophysiological recording and regulation of intracellular activities

Non-excitabile cells, lacking voltage-gated channels and are unable to detect changes in membrane potential from electrical input. However, their biological functions still require ionic transactions across the membrane, which itself generates signals that cause changes in membrane potential.

### 3. Fundamental Background

---

A helpful way to conceptualize the cell membrane with ionic channels is through an electrical circuit model [52,53]. The membrane can be represented by an electrical equivalent circuit, as depicted in Fig.3.3, where the switch symbolizes an ion channel.

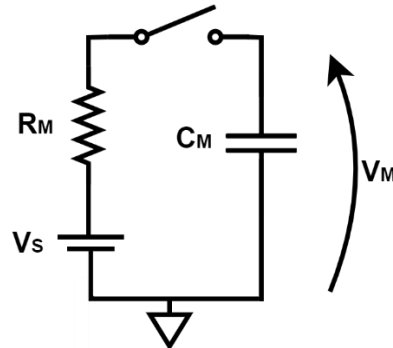


**Figure 3. 3** Membrane Equivalent Circuit

Where  $V_M$  represents the membrane potential,  $V_S$  serves as the battery source, symbolizing the ion gradient.  $R_M$  corresponds to the conductive pathway from the ion channel permeable to a particular ion species.  $C_M$  reflects the membrane's ability to store charge and the switch models the state of the ion channel, indicating whether it is open or closed. This is a simplified model representing just one ionic channel. This circuit is a passive RC circuit, meaning that the circuit can only respond to an applied electrical signal.

#### 3.3 Summary

In this chapter, we present a concise review of key concepts relevant to this thesis. These concepts primarily focus on how cells generate electrical fields and oscillations, as well as how they establish connections with neighbouring cells.

# Chapter 4

## Long-term stability of the electrical double-layer impedance

This chapter provides the fundamental background of the electrical double-layer established at the interface electrode/cell culture medium. It highlights the importance of the impedance parameters in controlling the SNR during electrophysiological sensing. It also discusses the long-term stability of the EDL during electrophysiological measurements.

## 4. Long-term stability of the electrical double-layer impedance

---

### 4.1. Introduction

The electrical double layer (EDL) forms at the interface between a conductive material and an electrolyte medium, creates a charged region at this boundary. Essentially, the EDL acts as a dipole layer, consisting of ions on the electrolyte side and electrons on the electrode side. It is a very thin layer, typically just a few nanometres thick. This dipole layer results in a high electrical impedance.

The impedance of the EDL can be effectively modelled as a parallel combination of capacitance and resistance (see Fig. 4.1). Alternating current (AC) signals flow primarily through the low-impedance capacitance ( $C_D$ ), while direct current (DC) signals pass through the parallel resistance ( $R_D$ ). In this thesis, only AC signals are used. For recording extracellular cell signals, maximizing the capacitance ( $C_D$ ) is critical, as higher capacitance reduces the impedance to AC signals. Meanwhile, the resistance component contributes to thermal noise, so minimising the interfacial resistance is essential to reduce noise and enhance the SNR.

The electrolyte medium supplies the ionic charges that contribute to the formation of the (EDL). Cell culture mediums, commonly used as electrolyte mediums, are highly complex in composition, containing various nutrients, antibiotics, and other components.

Extracellular electrophysiological measurements are often conducted over extended periods, lasting more than a day. Over such long durations, changes in the EDL may occur, potentially caused by the accumulation of materials or sedimentation on the electrode surface. These changes could affect the impedance of the EDL, altering the electrical parameters that influence the SNR. As a result, the SNR of the sensing electrodes may fluctuate over time rather than remaining constant.

The experiments described in this chapter are designed to evaluate the electrical stability of the EDL over several days, assessing whether any significant changes occur that could impact the reliability of the measurements.

This chapter begins by introducing the equivalent circuit that describes the frequency dependence of the electrode when immersed in an electrolyte medium. This equivalent circuit modelling aims to understand each circuit component's impact on the impedance. Using equivalent circuit modelling, we can associate different parts of the spectrum with specific electrode and cell culture medium regions. Specifically, it allows us to determine whether temporal variations occur near the electrode surface or in the

## **4. Long-term stability of the electrical double-layer impedance**

---

bulk electrolyte region. Next, we examine the temporal changes in impedance components for various types of cell culture mediums, ionic solutions, and complex mixtures with fructose.

### **The Electrical Double Layer**

The structure that forms at the interface between the electrode and the electrolyte, resulting from the separation of charges when ions from the electrolyte accumulate on the electrode's surface, creating a layer of electric charge at their boundary, is known as the Electrical Double Layer (EDL). The concentration of ions is highest at the point closest to the electrode, where the electrode's electrical influence is strongest. As you move further away from the electrode, the concentration of ions gradually decreases until it reaches the bulk concentration, which is the normal level found in the electrolyte when it is not under the influence of the electrode [54].

The EDL consists of two layers [55]. The first, called the Stern layer, results from the accumulation of counterions on the surface of the electrode, while the second layer, called the Gouy-Chapman layer, results from the diffusion layer extending outward from the Stern surface.

The Stern layer, also known as the Helmholtz layer, is the region closest to the electrode surface where counterions accumulate directly due to the strong electrostatic attraction from the charged electrode. In this layer, the ions are tightly bound and do not move freely, forming a compact layer that partially neutralizes the electrode's surface charge. The Stern layer acts similarly to a capacitor, where the ions create a sheet of charge that closely balances the electrode's charge.

The Gouy-Chapman layer is a diffuse layer that extends outward from the Stern layer into the electrolyte solution. In this layer, the ions are more loosely distributed and not fixed in place, with their concentration gradually decreasing as the distance from the electrode increases. This layer represents a balance between the electrostatic attraction towards the electrode and the thermal motion that causes the ions to spread out.

### **Extracellular signals recording**

The recording of signals with extracellular electrodes are called extracellular signals, since there is no invasion of the cell body and the signal detection inherently depends

## 4. Long-term stability of the electrical double-layer impedance

both on the electrode properties and on the coupling properties of the cell membrane to the electrodes, that is, the adhesion of the cell membrane to the sensing electrode.

Since the entire cell body is bathed in an electrolyte, the regions between the cell membrane and the electrode are filled with this electrolyte, creating a complex electrical circuit.

Assuming that  $i(t)$  is a time varying signal composed by a cooperative action between cells that is given by the sum of all the currents emanating from all the cells that cover the sensing electrode, resulting in a potential drop in the sensor electrode ( $V_S(t)$ ) equivalent to the extracellular signal potential. In this situation, an equivalent circuit model can be derived for a system comprised by two parallel electrodes, of which one electrode acts as the measuring (also referred as sensing electrode) and the other as the counter electrode, to describe the electrode/electrolyte interface considering the presence of living cells covering the device surface, shown in Figure 4.1.

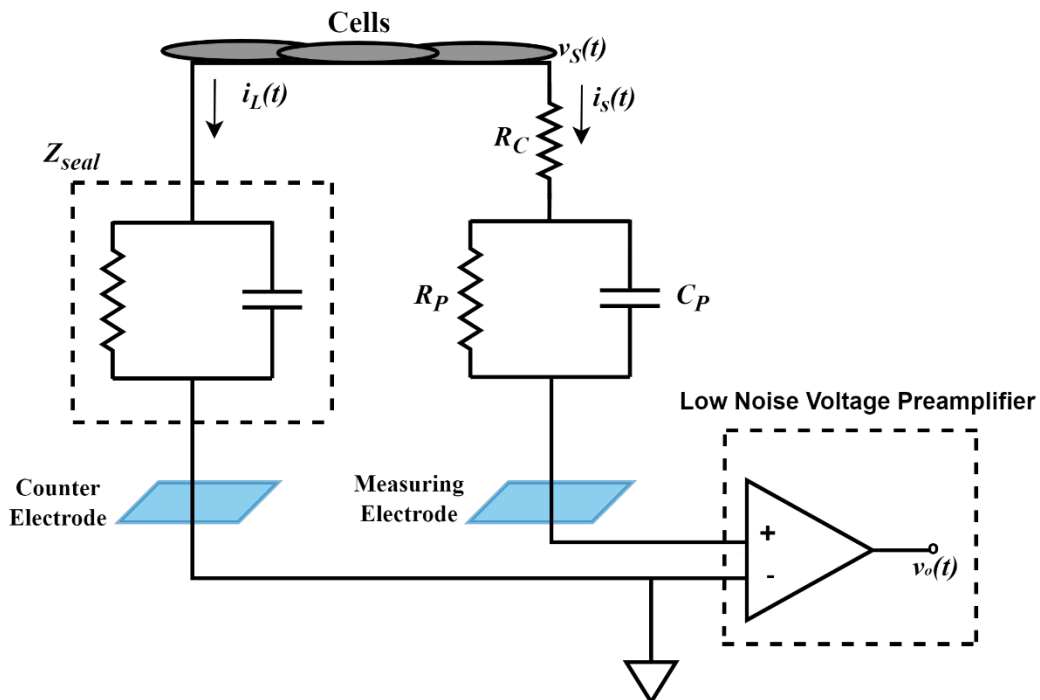


**Figure 4. 1** Illustration of the electrical coupling of extracellular signals detected with microelectrodes.

Detailing each element in Figure 4.1:  $i_L(t)$  represents the current generated by the cells, which flows through the electrolyte sealing impedance and  $i_S(t)$  represents the current generated by the cells that flow through the measuring electrode impedance.  $V_S(t)$  is



## 4. Long-term stability of the electrical double-layer impedance

the extracellular signal potential generated by the current within the system and  $V_o(t)$  is the output signal from the voltage preamplifier.

The spreading resistance ( $R_C$ ) represents the loss of signal as it spreads through the electrolyte from the cell to the electrode.  $C_P$  and  $R_P$  represent the electrical double layer at the electrode-electrolyte interface. The seal impedance ( $Z_{SEAL}$ ) is formed by the electrolyte impedance in series with the counter electrode double-layer impedance.

The measuring circuit is completed with the low-noise voltage preamplifier.

When cells are in contact with the measuring electrode, the signal loss between the cell and the measuring electrode is modelled by the resistance  $R_C$ . It is important that  $R_C$  is small, this ensures that the extracellular signal is essentially coupled into the measuring electrode:

$$R_C \ll Z_{SEAL}$$

### EDL circuit modelling

From an electrical perspective, the EDL in series with the electrolyte can be effectively modelled by an equivalent RC network. Figure 4.2 depicts a common model applied to represent the electrode-electrolyte interface, known as the Randles and Somerton model [56].

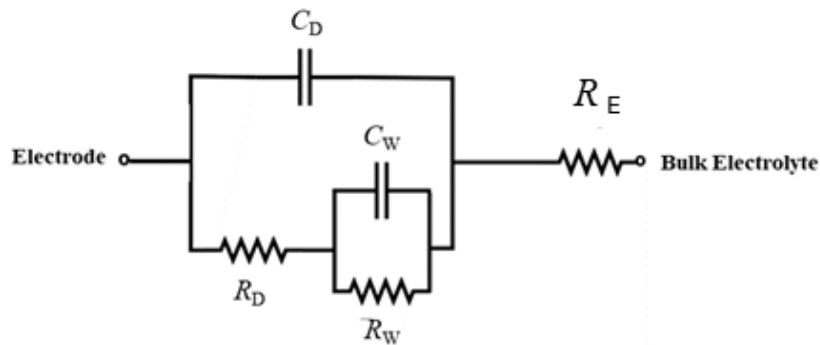


Figure 4. 2 Randles and Somerton electrode-electrolyte model.

This model accounts for the interfacial capacitance of the EDL ( $C_D$ ) in parallel with the interfacial charge transfer resistance of the EDL ( $R_D$ ) and to the diffusion related

## 4. Long-term stability of the electrical double-layer impedance

Warburg element, here shown as the parallel RC circuit combination between  $R_W$  and  $C_W$ .  $R_E$  represents the electrolyte resistance, which is related to the effect of current spreading from the electrode to the counter electrode.

The purpose of carrying out the simulation using an equivalent circuit is to identify the changes in the impedance with the physical location where they occur. For the purposes of recording extracellular signals, the contribution of the Warburg element is small. Therefore, we decided to simplify the equivalent circuit and to remove the Warburg element.

However, we add a parallel capacitance with the bulk electrolyte resistances. The circuit used to simulate the EDL in series with a neutral bulk layer is shown in Figure 4.3a.

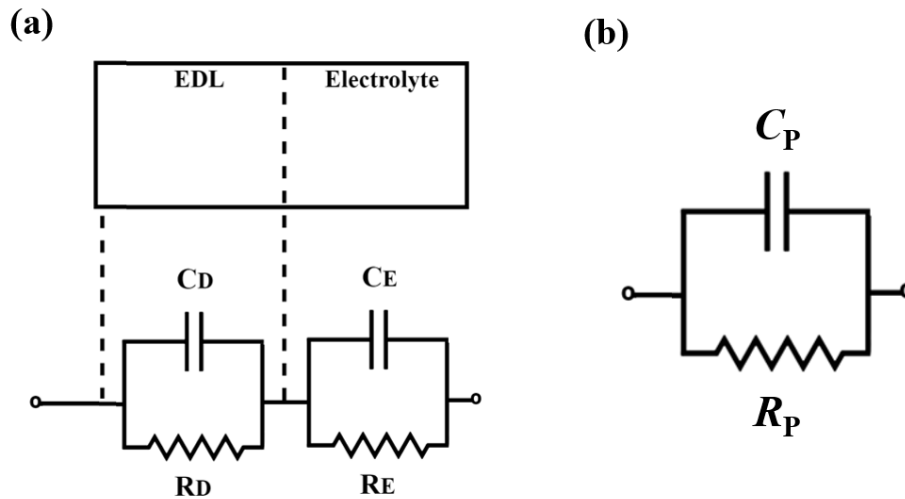


**Figure 4.3** (a) Double RC circuit used to describe electrodes immersed into an electrolyte system (b) Equivalent Circuit assumed by the impedance analyzer. The impedance analyser measures  $C_P$  and  $R_P$ , which are related to the equivalent circuit that describes the system.

The EDL is in series with the bulk electrolyte layer. The bulk electrolyte layer is formed by the parallel network comprised by the bulk electrolyte resistance ( $R_E$ ) and capacitance ( $C_E$ ).

The impedance analyser assumes that the physical system that is measuring is a parallel RC circuit. Therefore, the experimental readings are  $R_P$  and  $C_P$  values that should be related to the simplified equivalent circuit as shown in the Figure 4.3 (b).

The admittance of the EDL layer is

## 4. Long-term stability of the electrical double-layer impedance

$$Y_{DL} = \frac{1}{R_{DL}} + j\omega C_{DL} \quad (4.1)$$

The admittance of the bulk electrolyte layer  $Y_E$  given by

$$Y_E = \frac{1}{R_E} + j\omega C_E \quad (4.2)$$

$Y_{DL}$  is in series with  $Y_E$ , therefore the combination of the two is a total admittance  $Y_T$  given by series combination of  $Y_{DL}$  with  $Y_E$

$$Y_T = \frac{Y_{DL} + Y_E}{Y_{DL} Y_E} \quad (4.3)$$

Now this admittance must be expressed in terms of a  $R_P$  and a  $C_P$  values which are the values measured by the impedance analyser

$$Y_T = \frac{1}{R_P} + j\omega C_P \quad (4.4)$$

We can then extract the  $C_P$  and  $R_P$  values:

$$C_P = \frac{\text{Imag}(Y_T)}{\omega} \quad (4.5)$$

$$R_P = \frac{1}{\text{Real}(Y_T)} \quad (4.6)$$

When plotting the frequency response of the systems is convenient to plot not  $R_P$  but the value of  $1/(\omega R_P)$  which is named *Loss*. The *Loss* parameter is convenient because it provides a maximum where the two-layer system has a relaxation [57]. Furthermore, *Loss* and capacitance have the same units (Farad).

The above relationship were implemented in a MATLAB script to simulate the frequency response of the circuit. To inspect the contribution of each element each circuit was varied individually. Below it is represented the changes on the frequency response of the electrode/electrolyte systems.

## 4. Long-term stability of the electrical double-layer impedance

### 4.2. Methodology and experiments

#### 4.2.1. Experimental setup

The system designed for recording ultra-weak signals from non-electrogenic cells includes a low-noise preamplifier directly coupled to the transducer device. This preamplifier amplifies the signals, which are then sent to an oscilloscope for proper visualization, with the time scale carefully adjusted to capture the nuances of the signal.

Once data acquisition is complete, the files are transferred to a computer for further processing. The schematic diagram of the system is shown in Figure 4.3 and the real acquisition signals system components are shown in Figure 4.4.

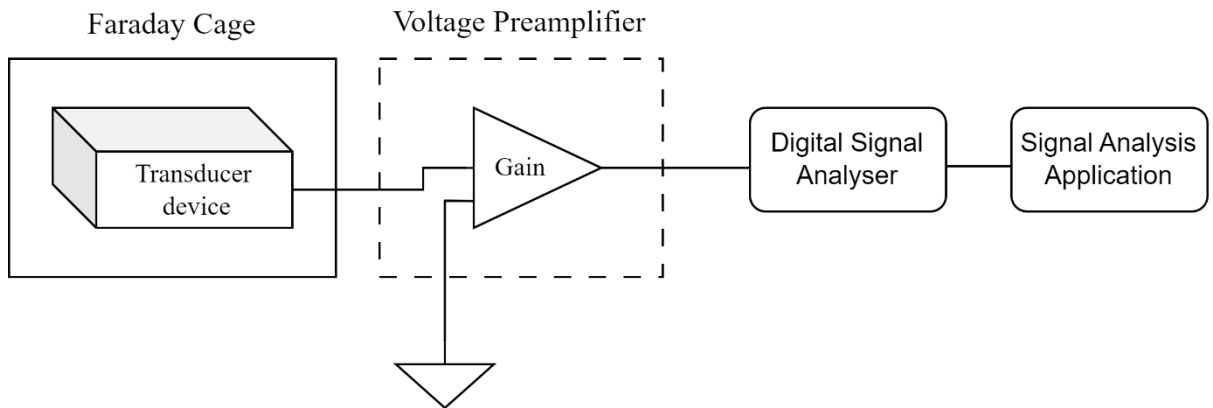


Figure 4. 4 Acquisition signals system illustration



Figure 4. 5 Acquisition signals system components: Voltage preamplifier; Digital Signal Analyser; Computer using application for signal analysis

Small signal impedance measurements were carried out using an impedance analyser, Fluke PM6306 (Fluke Corporation, Everett, USA). A self-developed software

## **4. Long-term stability of the electrical double-layer impedance**

called RCL, which runs only on Microsoft computers, was used to remotely control, and perform all measurements in this work. The RCL software runs on Microsoft computers.

The connection of the electrodes to the measuring device was made using gold wire, positioned with the help of liquid silver, both materials with extremely high conductivity. After the connection of the transducer device, the samples were placed within a die-cast aluminium case. The case was then placed inside an incubator to maintain a constant temperature of 37°C, ensuring that this condition did not affect the results.

To protect the recording system from electromagnetic interference, it was placed inside a 1-meter cube-shaped Faraday cage made of 5 mm thick iron, which was positioned on top of anti-vibrational mounts at each corner.

### **4.2.2. Electrodes**

The electrodes used are based on standard technology, the commercial 8 Well PET Arrays purchased to Applied Biophysics, New York, USA, consisting of patterned gold electrodes on a polyethylene terephthalate (PET) substrate. [58]

All samples contain 8 well PET arrays and have the same pattern of electrodes per well. The gold tracks between the electrodes and larger contact pads are insulated with a thin layer of cured photoresist polymer.

A well PET array has a single circular electrode with a diameter of 250  $\mu\text{m}$  located in the centre, resulting in a total electrode area ( $A_e$ ) of 0.049  $\text{mm}^2$  and spacing 3mm to the counter electrode.

### **4.2.3- Culture Media**

To evaluate the influence of the electrolyte composition on the impedance behaviour of the test circuit used, 5 different types of culture media were used, namely: Dulbecco's Modified Eagle Medium (DMEM); Kaighn's Modification of Ham's F-12 Medium (F12K); a medium consisting only of fructose and KCl studied at two different KCl concentration (KCl 10mM; fructose 20% and KCl 6mM; fructose 20%), and a medium containing only KCl at a concentration of 16mM.

Dulbecco's Modified Eagle Medium (DMEM)[59] is a widely used basal medium for supporting the growth of many different mammalian cells. Astrocytes have been

## 4. Long-term stability of the electrical double-layer impedance

proven to be compatible with this type of medium. It is a sugar-rich medium and contains an extensive list of amino acids and vitamins, besides glucose and inorganic salts.

F12-K [60] is also a widely used complex medium in biological studies. Compared to DMEM, it has a more extensive and varied list of salts, but in very similar concentrations. The main difference between these two media is indeed the amount of sugar, with F12-K containing about one quarter of the sugar content found in DMEM.

The initial media studied, DMEM and F12-K, as said before, are complex formulations that include a wide range of components. To investigate the specific effects of individual components, simpler media containing only fructose and KCl was also examined. This approach allows us to analyse the influence of these components, such as proteins.

To explore how salt concentrations impact the EDL compartment, two media were prepared containing only fructose and KCl but with different concentrations of the salt. Finally, a medium containing only KCl, without any sugar source, was used to assess the salt influence in impedance.

### 4.2.4 Experience Description

The general settings were the following, the test signal (AC level) used was a voltage field with an amplitude of 100 mV AC and a bias component of 0 V DC and the test circuit used was a parallel resistor-capacitor admittance circuit ( $R_P \parallel C_P$ ).

## 4.3. Results

### 4.3.1. Design Rules

Using the circuit model from Figure 4.4, to understand the influence on both the capacitance and the loss of the system, the values of each component were varied while keeping the others constant. The initial model is shown in Figure 4.5, and the components had the following values:  $C_D = 3 \text{ nF}$ ;  $R_D = 3 \text{ M}\Omega$ ;  $C_E = 0.5 \text{ nF}$ ;  $R_E = 3 \text{ k}\Omega$ . Figures from 4.6 to 4.9 show the influence of  $C_D$ ,  $R_D$ ,  $C_E$  and  $R_E$  respectively.

## 4. Long-term stability of the electrical double-layer impedance

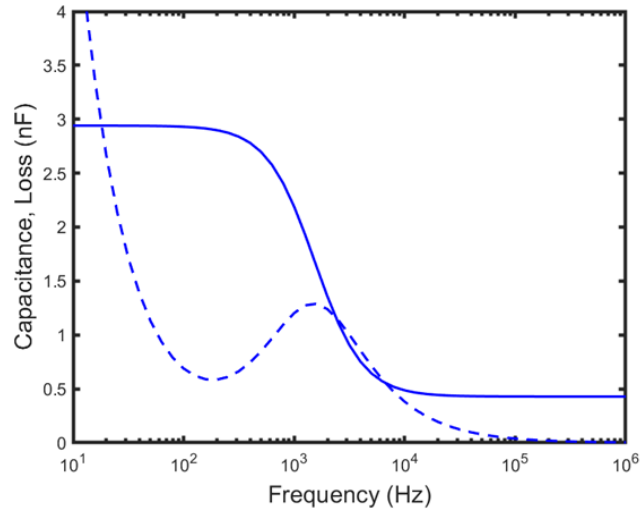


**Figure 4. 6** Equivalent circuit (Fig. 4.3a) frequency response.

(a) EDL frequency response when  $C_D$  changes

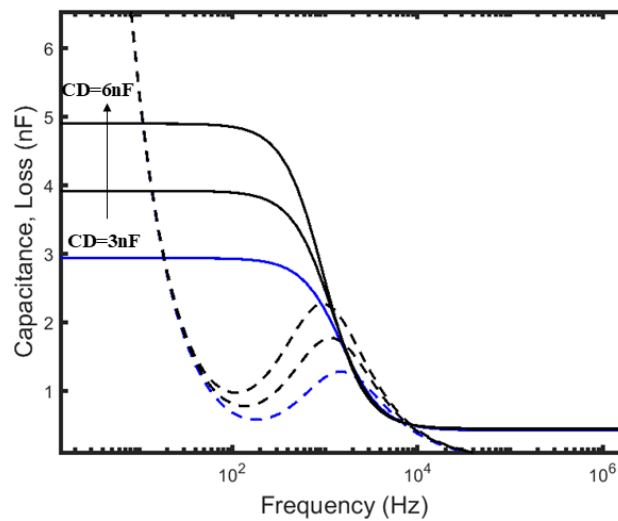


**Figure 4. 7** Frequency response with multiple values for the  $C_D$  component:  $C_D = 3\text{nF}$  (initial),  $C_D = 4.5\text{nF}$ ,  $C_D = 6\text{nF}$  (see circuit in Fig. 4.3a)

(b) EDL frequency response when  $R_D$  changes

## 4. Long-term stability of the electrical double-layer impedance

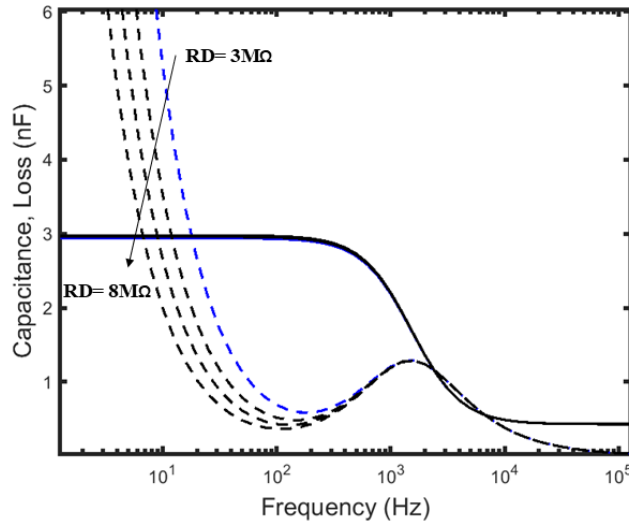


**Figure 4. 8** EDL frequency response with multiple values for the  $R_D$  component:  $R_D = 3\text{M}\Omega$  (initial),  $R_D = 4.5\text{M}\Omega$ ,  $R_D = 6\text{M}\Omega$ ,  $R_D = 8\text{M}\Omega$

(c) EDL frequency response when  $C_E$  increases

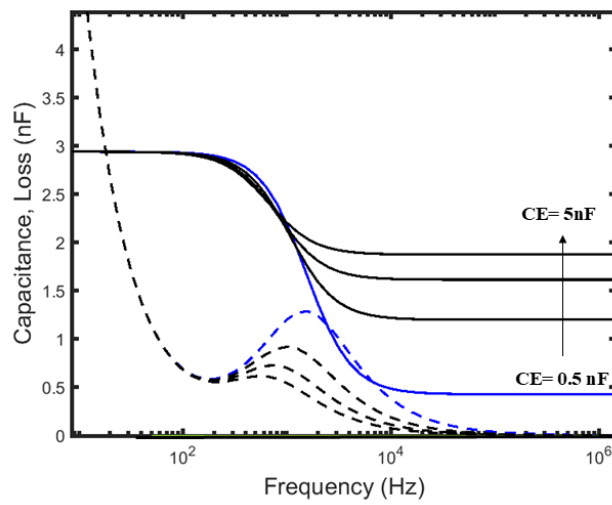


**Figure 4. 9** EDL frequency response with multiple values for the  $C_E$  component:  $C_E = 0.5\text{nF}$  (initial),  $C_E = 2\text{nF}$ ,  $C_E = 3.5\text{nF}$ ,  $C_E = 5\text{nF}$

(d) EDL frequency response when  $R_E$  changes



## 4. Long-term stability of the electrical double-layer impedance

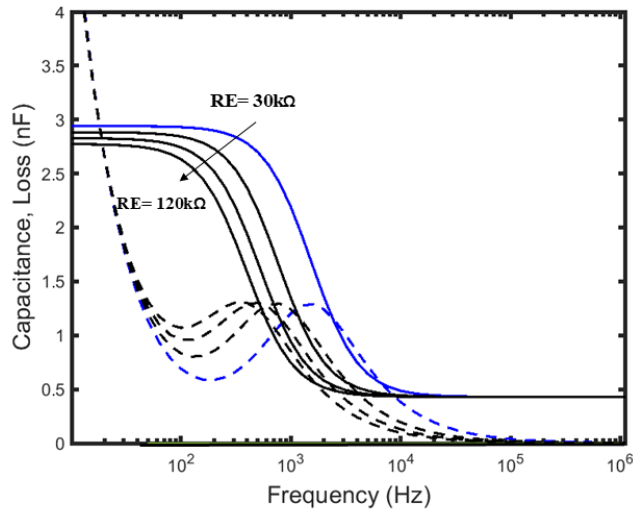


**Figure 4.10** EDL frequency response with multiple values for the  $R_E$  component:  $R_E = 30\text{k}\Omega$  (initial),  $R_E = 60\text{k}\Omega$ ,  $R_E = 90\text{k}\Omega$ ,  $R_E = 120\text{k}\Omega$

### 4.3.2. Media Results

Samples of different electrolytes were prepared and placed on the electrodes. These results show the measurement of loss and capacitance of these same samples over frequency, before and after a certain period.

#### (a) DMEM media

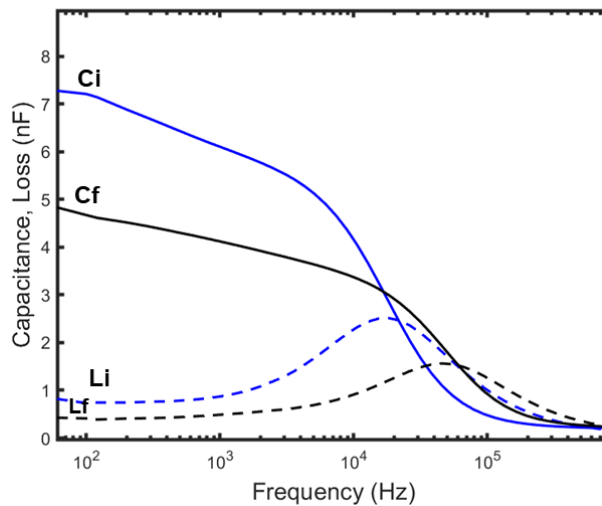


**Figure 4.11** Comparison of the capacitance and loss at the beginning ( $t=0\text{h}$ ) ( $C_i$  and  $L_i$ ) and at the end ( $t=42.7\text{h}$ ) ( $C_f$  and  $L_f$ ) of the experiment with DMEM media.

#### (b) F-12K media

## 4. Long-term stability of the electrical double-layer impedance

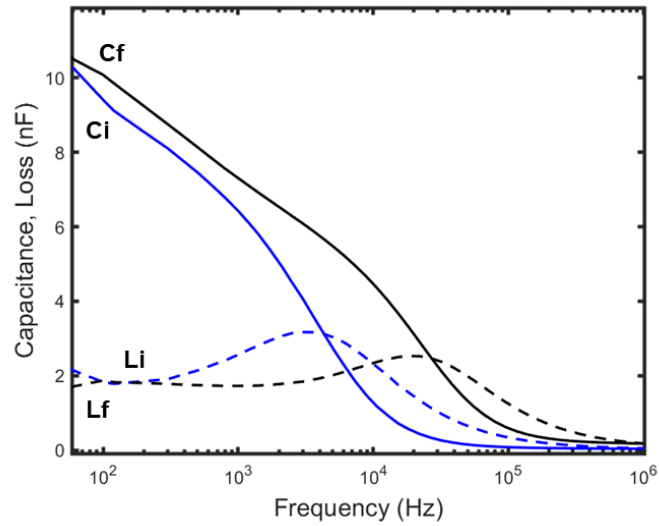


**Figure 4. 12** Comparison of the capacitance and loss at the beginning ( $t=0h$ ) ( $C_i$  and  $L_i$ ) and at the end ( $t=43.4h$ ) ( $C_f$  and  $L_f$ ) of the experiment with F-12K media.

**(c) Media containing KCl (10mM) and Fructose (20%).**

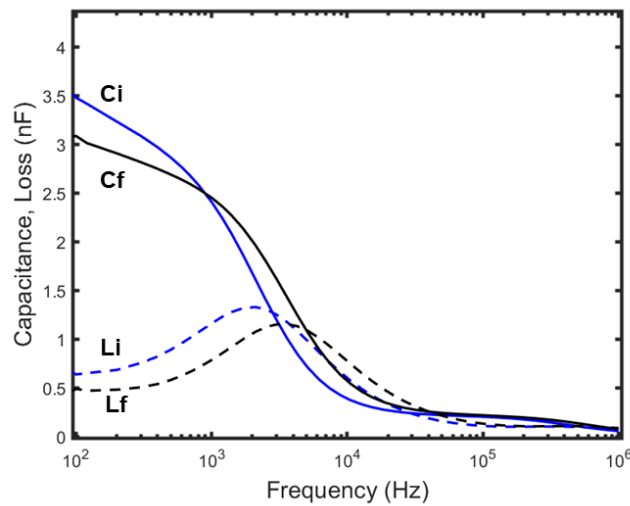


**Figure 4. 13** Comparison of the capacitance and loss at the beginning ( $t=0h$ ) ( $C_i$  and  $L_i$ ) and at the end ( $t=45.4h$ ) ( $C_f$  and  $L_f$ ) of the experiment with media containing KCl 10mM and Fructose 20%.

**(d) Media containing KCl (6mM) and Fructose (20%).**

## 4. Long-term stability of the electrical double-layer impedance

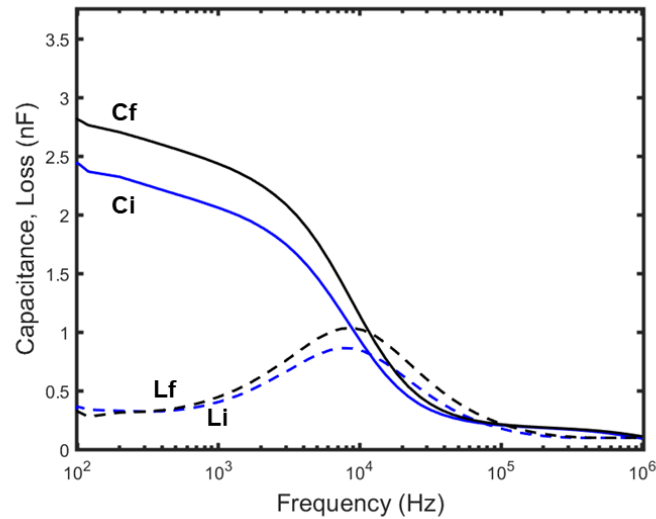


**Figure 4. 14** Comparison of the capacitance and loss at the beginning ( $t=0h$ ) ( $C_i$  and  $L_i$ ) and at the end ( $t=33.6h$ ) ( $C_f$  and  $L_f$ ) of the experiment with media containing KCl 6mM and Fructose 20%.

### (e) Media containing KCl 16mM.

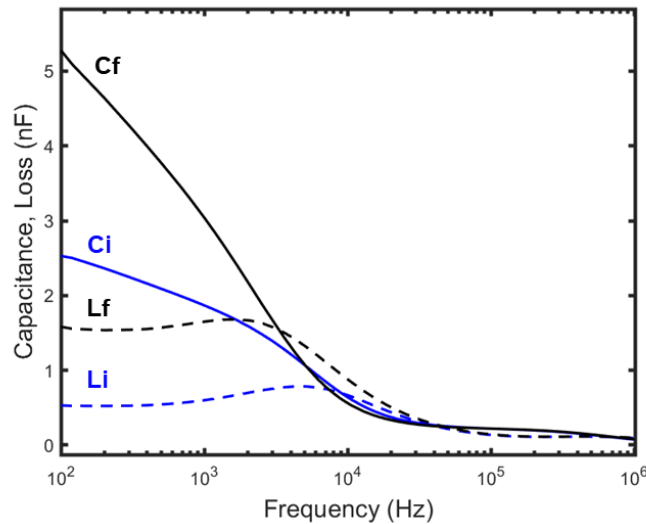


**Figure 4. 15** Comparison of the capacitance and loss at the beginning ( $t=0h$ ) ( $C_i$  and  $L_i$ ) and at the end ( $t=34.2h$ ) ( $C_f$  and  $L_f$ ) of the experiment with media containing KCl 16mM.

### 4.4. Discussion

In Figure 4.2, a model circuit featuring a component known as the Warburg element was presented. As said before, for simplification, this element's effect was disregarded during signal acquisition and analysis. However, the influence of this element is

## 4. Long-term stability of the electrical double-layer impedance

still noticeable, though not critical,. The influence of this element is visible in the initial curvature of the capacitance, whereas in the model, it appears as a straight line.

For each electrolyte medium, we can conclude the influence that time had on the behaviour of impedance, given that these measurements were taken at significant intervals of 34h to 48h. By visualizing the graphs, comparing the values at the beginning of the experiment and several hours later, and considering the influence of each component on the final design of the graphs, Table 4.1 was elaborated.

**Table 4. 1** Time influence on the values of each component

	$C_E$	$R_E$	$C_D$
DMEM	+	-	-
F-12k	-	-	+
KCl 10mM +fructose 20%	-	-	-
KCl 6mM + fructose 20%	=	=	+
KCl 16mM	+	+	+

The influence on impedance of the sugar/carbohydrate, inorganic salts and proteins/vitamins can be concluded by comparing media with similar characteristics that differ only in the constituent being studied.

The sugar influence can be analysed by comparing the following media: DMEM with F-12K; media containing KCl 10mM and Fructose 20% with media containing KCl 16mM.

In media with higher sugar content (DMEM and KCl (10mM)),  $C_P$  decreases, while in media with lower sugar content,  $C_P$  increases, a trend observed in both comparisons. Additionally,  $C_E$  in media with higher sugar is greater than in media with lower sugar, and  $C_D$  in media with higher sugar is lower than in media with less sugar. The relaxation point remains unchanged, indicating that sugar does not affect  $R_E$ .

Regarding the influence of proteins and vitamins, comparing the media: DMEM with media containing KCl 10mM and Fructose 20%; and F-12K with media containing KCl 10mM and Fructose 20%. There is a slight decrease in  $R_E$  in the medium containing only salt and sugar when compared to more complex media, but this variation is not significant. Therefore, no visible influence is observed comparing both experiments that

## **4. Long-term stability of the electrical double-layer impedance**

cannot be explained by the presence of other constituents like salts and sugars in each medium.

For salt influence, by comparing the media containing KCl 10mM and Fructose 20% with the media containing KCl 6mM and Fructose 20%.

The media with a higher salt concentration shows significantly higher  $R_E$  values, meaning that relaxation occurs at low frequencies, while in the lower salt concentration media, relaxation occurs at higher frequencies. There is no concrete influence of salt on the other components.

### **4.5. Conclusions**

The conclusion is that the constituents of the electrolytic medium interfere with the system's capacitance and overall loss of the electrode/electrolyte system.

The presence of proteins and other typical constituents of culture media does not appear to significantly alter the impedance and the frequency response. However, both the presence and concentration of sugars and salt have an influence. The presence of sugar seems to affect the capacitive components of the circuit. The most notable influence comes from salt, which increases the bulk electrolyte conductivity and causes a shift in the relaxation of the loss.

# Chapter 5

## Extracellular Astrocyte Signals: The role of the electrode geometry on the signal duration

This chapter addresses fundamental aspects related to the nature of the bioelectrical signals generated by astrocyte populations. Connected populations of astrocytes can generate not only electrical noise but also discrete electrical oscillations. It is important to know if these oscillations are travelling waves or steady-state oscillations generated by a cluster of cells that synchronize their activity. This chapter aims to gain insight into the type of electrical oscillation generated by astrocyte populations.

## 5. Extracellular Astrocyte Signals

### 5.1. Introduction

It is widely accepted that individual astrocytes cannot generate discrete signals such as APs. However, numerous studies suggest that astrocyte populations cooperate and synchronize their activity to produce waves that propagate across tissues or compact cell monolayers. These are commonly referred to as calcium waves [61]

Although calcium oscillations occur within astrocytes, they may also produce an extracellular component that can be detected by external electrodes. Calcium waves typically propagate at speeds of 10-50 microns per second [62], and the duration of calcium waves in astrocytes is described as being in the range of several seconds to tens of seconds [63]. These waves are commonly visualized through optical microscopy using calcium fluorescence probes. However, it is crucial to understand how these waves can be detected electrically by extracellular electrodes instead of relying on optical methods.

Figure 5.1 illustrates the concept of using electrodes to detect travelling waves. As a wave passes over an electrode, it generates a transient rise in cell potential, lasting as long as the wave takes to cross the electrode. Narrow electrodes capture brief oscillations, whereas wider electrodes record longer voltage oscillations. Therefore, voltage signals of varying durations can be obtained by designing electrodes with different widths.

Our conceptual view of wave-crossing electrodes predicts the observation of square-like voltage signals. The bioelectrical signals recorded are biphasic. Therefore, they do not entirely fit with our view. The biological mechanism behind the shape of these signals is not clear yet.

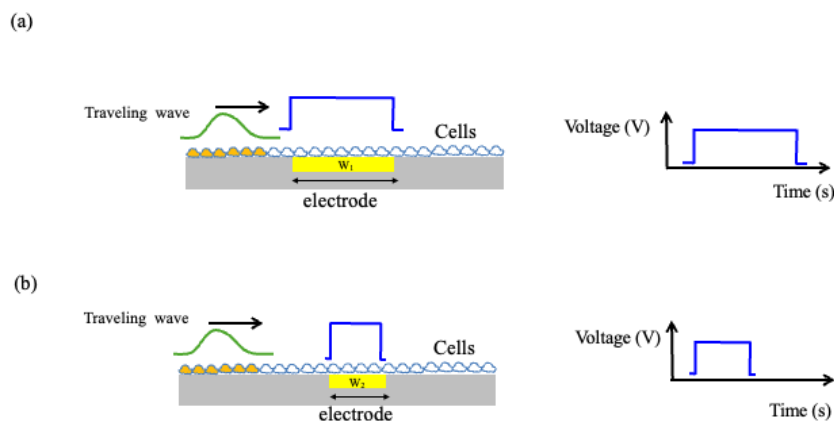


**Figure 5. 1** Conceptual view of recording a travelling wave using extracellular electrodes. (a) wave crossing an electrode with width  $W_1$ . (b) A wave crossing a shorter electrode with width  $W_2$ .

## 5. Extracellular Astrocyte Signals

---

In addition to the electrode geometry to inspect for travelling waves, simple round electrodes with different areas were fabricated and used to record extracellular signals and to inspect the effect of the electrode area on the signal duration and the signal power.

The objective of this experiment is to observe discrete signals arising from synchronised cellular activity. Specifically, the focus is on a cluster of cells working together to produce an electrical oscillation. Unlike travelling waves, this oscillation remains localised within the cell cluster that generates it. Currently, there is no information regarding the number of cells that can participate in this synchronisation or the spatial extent of the cluster. If this mechanism is operating, it can be hypothesised that the recorded signal strength (or power) will also increase as the number of synchronised cells increases.

Small-area electrodes inherently limit the size of the cell clusters that can be measured, with the maximum cluster size constrained by the electrode's surface area. In contrast, larger-area electrodes can accommodate larger clusters. As a result, we expect to observe a broader distribution of signal strengths with larger-area electrodes. This relationship between electrode size and signal power distribution assumes that the area of the smallest electrodes is smaller than the dimensions of the largest synchronised cell clusters.

This chapter presents the fabricated electrode designs and the corresponding electrical signal records. The analysis involves a selection of discrete signals with well-defined shapes that allow quantifying the signal duration.

### 5.2. Methods

#### (a) Electrodes

The electrophysiological system used to record bioelectrical activity is described in detail in Chapter 3. All recordings were conducted in voltage mode.

To examine the electrode's role in controlling signal duration and power, two electrode geometries were tested. One configuration, shown in Figure 5.2, features concentric circular fingers with varying widths.



## 5. Extracellular Astrocyte Signals

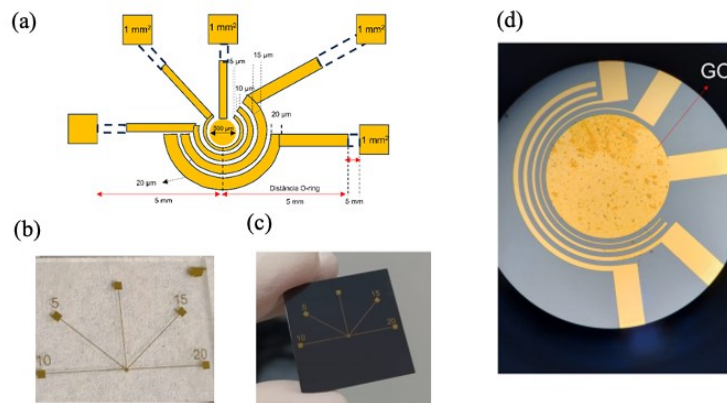


**Figure 5.2** Patterns of circular concentrating rings with different widths. (a) schematic diagram with the dimensions. (b) Gold electrode fabricated in a glass substrate. (c) electrode pattern fabricated on a thermally oxidized silicon wafer. (d) A photograph of the central region clearly shows the electrodes.

The electrodes provided by Applied Biophysics<sup>TM</sup> feature patterned gold on a polycarbonate (PET) substrate. This electrode type is particularly well-suited for studying the impact of electrode area on signal power. The circular electrode is coated with a polymer layer that can be selectively removed using a diluted solution of NaOH. By adjusting the size of the NaOH droplet in contact with the polymer, different areas of the underlying gold electrode can be exposed. This method offers a simple and effective way to create electrodes with varying active surface areas.

The electrode area was varied from 0.08 cm<sup>2</sup> to 0.23 cm<sup>2</sup>. Figure 5.3 presents the commercial electrodes obtained from Applied Biophysics, along with a schematic diagram of the electrode design.

## 5. Extracellular Astrocyte Signals

---

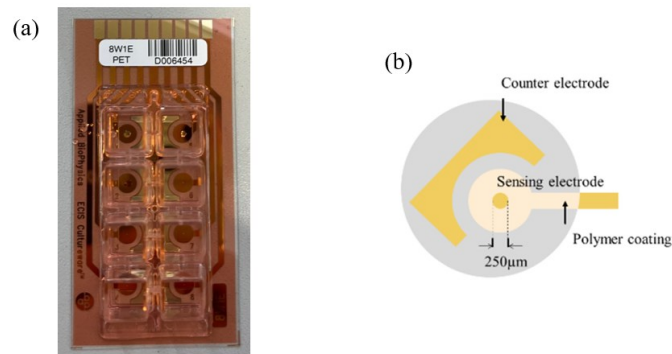


**Figure 5.3** (a) Commercially available electrodes from applied Biophysics (ref. 8W1E PET) device with 8 wells. (b) Schematic representation of the electrode geometry.

### (b) Cells

The astrocytes (c8d1a- Astrocyte type I clone) [64] used are astrocytes isolated from the cerebellum of mice. Cells were cultured in the laboratory using DMEM medium, previously described in Chapter 3. For accurate measurements to be taken, it is essential that all biological conditions are met, including cell confluence and the formation of a uniform monolayer.

## 5.3. Results

### 5.3.1 Electrophysiological time traces

Electrophysiological time traces were recorded over several days. Figure 5.4 provides an overview of a long-duration experiment. Overall, the activity is characterised by periods of intense activity, often consisting of discrete signals interspersed with quieter intervals.

## 5. Extracellular Astrocyte Signals

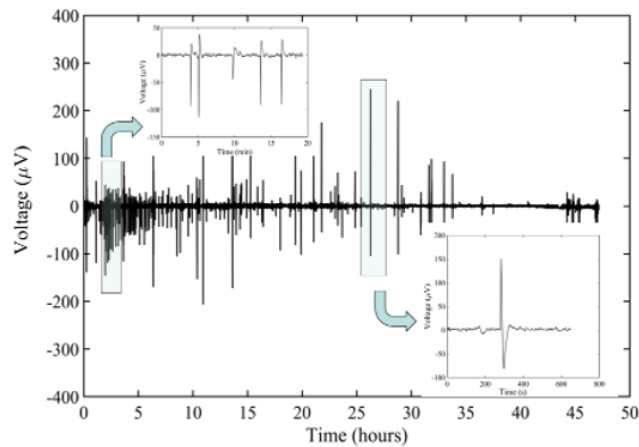


**Figure 5. 4** Electrical signals captured from a population of astrocytes, an overview of a long-term experiment.

### 5.4. Signal analysis

When cultured astrocytes are interfaced with MEAs, the electrical signals recorded from these cells can be categorised into three distinct types: biphasic signals, monophasic upward signals, and monophasic downward signals. Biphasic signals are the most prevalent and easy to characterize. Biphasic signals are characterised by a waveform that exhibits two distinct phases. Two typical examples of biphasic signals are depicted in Figure 5.5. To quantify the signal's duration, the fast component of the signal (marked as  $\Delta t$  in Fig.5.5) was selected. Although  $\Delta t$ , is not the total signal duration, we found that it is simpler to quantify only the fast signal component than the entire signal component.

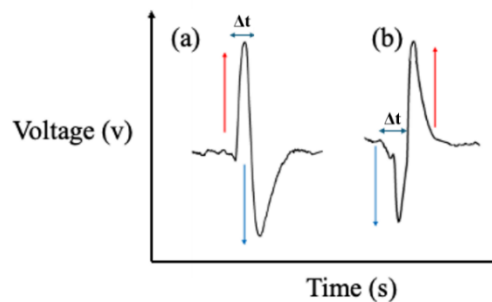


**Figure 5. 5** Typical shapes of biphasic signals recorded in astrocyte populations. The duration  $\Delta t$  of the short signal component was used as a quantification parameter to define the signal duration.

## 5. Extracellular Astrocyte Signals

---

The signal duration was selected as a good indication of the signal power; longer signals tend to have higher power. Figure 5.6 shows an example of this behaviour. However, since we do not know the biological origin of the fast signal component, it is questionable that the duration of the fast component is an adequate indicator to establish a relation with the area and geometry of the electrodes.

During a long-duration experiment, several biphasic signals are recorded. The duration of each signal was measured and grouped, and the durations were analysed to assess the activity of intercellular communication among astrocytes. Additionally, a study was conducted to determine whether the signal duration depends on the electrode's area and geometry, providing further insights into the factors influencing these bioelectrical events.

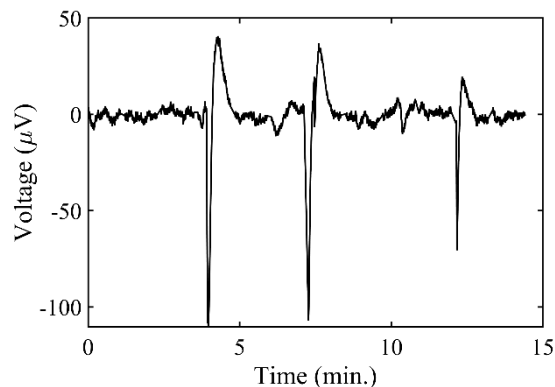


**Figure 5. 6** Typical biphasic signals in an astrocyte population.

### 5.5. Dependence of the signal duration on the area and geometry of the electrode

We identified many discrete signals across all the electrode areas and geometries described above in the long-term electrophysiological time traces. We measured the specific duration of each signal and found that they ranged from less than one second up to a maximum of 40 seconds. To properly describe this wide distribution of signal durations, we grouped the signals into bins with a duration of 1 second. Then, we counted the number of signals with durations fitting into each interval and represented this information as a histogram. The histograms for the 4 electrode widths are shown in Figure 5.6.

The 20- and 5-micron-width electrodes recorded a relatively high number of signals. However, the 5- and 15-micron electrodes captured relatively few discrete signals.

## 5. Extracellular Astrocyte Signals

---

In both cases, most signals had durations of less than 5 seconds, while signals lasting longer than 10 seconds were rare across all electrodes.

This signal dependence on the electrode width presented above suggests that electrode width does not significantly influence signal duration. Consequently, the data implies that the recorded signals do not align with the characteristics of a travelling oscillation or that the model assumed and described in the introduction section is incorrect.

A similar analysis of signal distribution was also carried out for the round electrode geometry, represented in Figure 5.8. Four different electrode areas were used. The maximum of the distribution peaks in signal durations is below 5 seconds. Signals longer than 10 seconds are rare in all the electrode areas.

## 5. Extracellular Astrocyte Signals

---

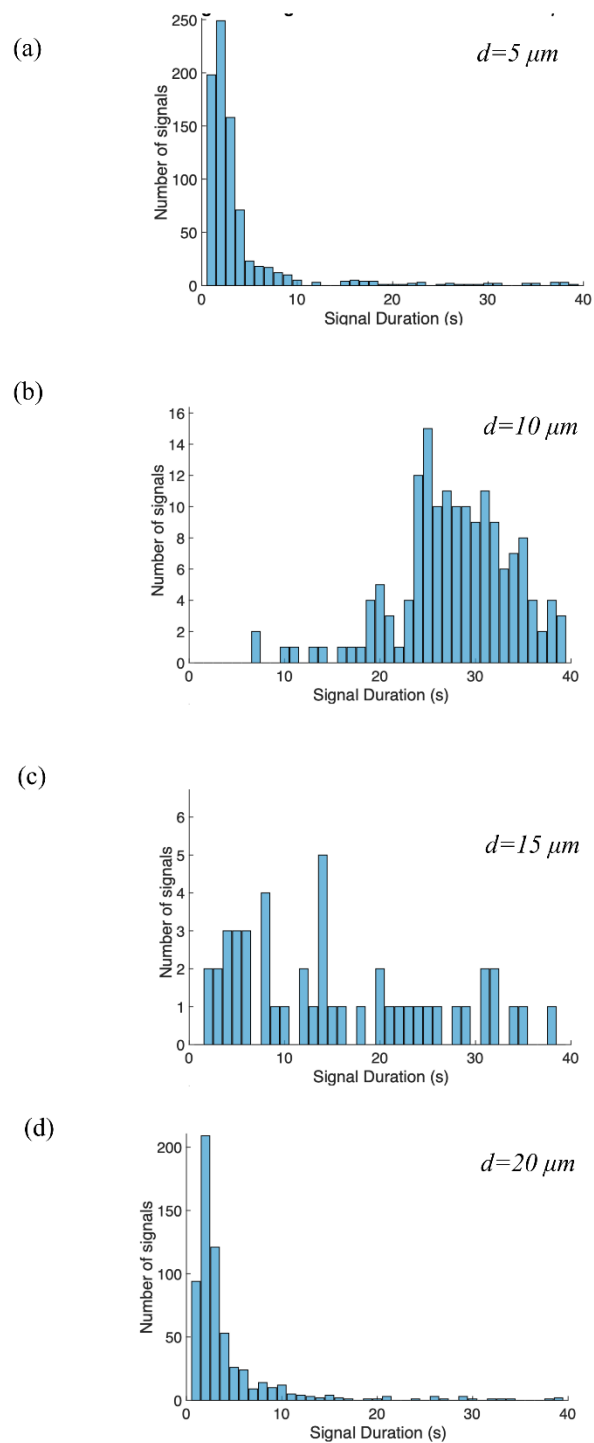


**Figure 5. 7** Comparison of signal duration for circular electrodes with different electrode widths. Electrode geometry is represented in Figure 5.2.  $d$  being the width of the electrode.

## 5. Extracellular Astrocyte Signals

---

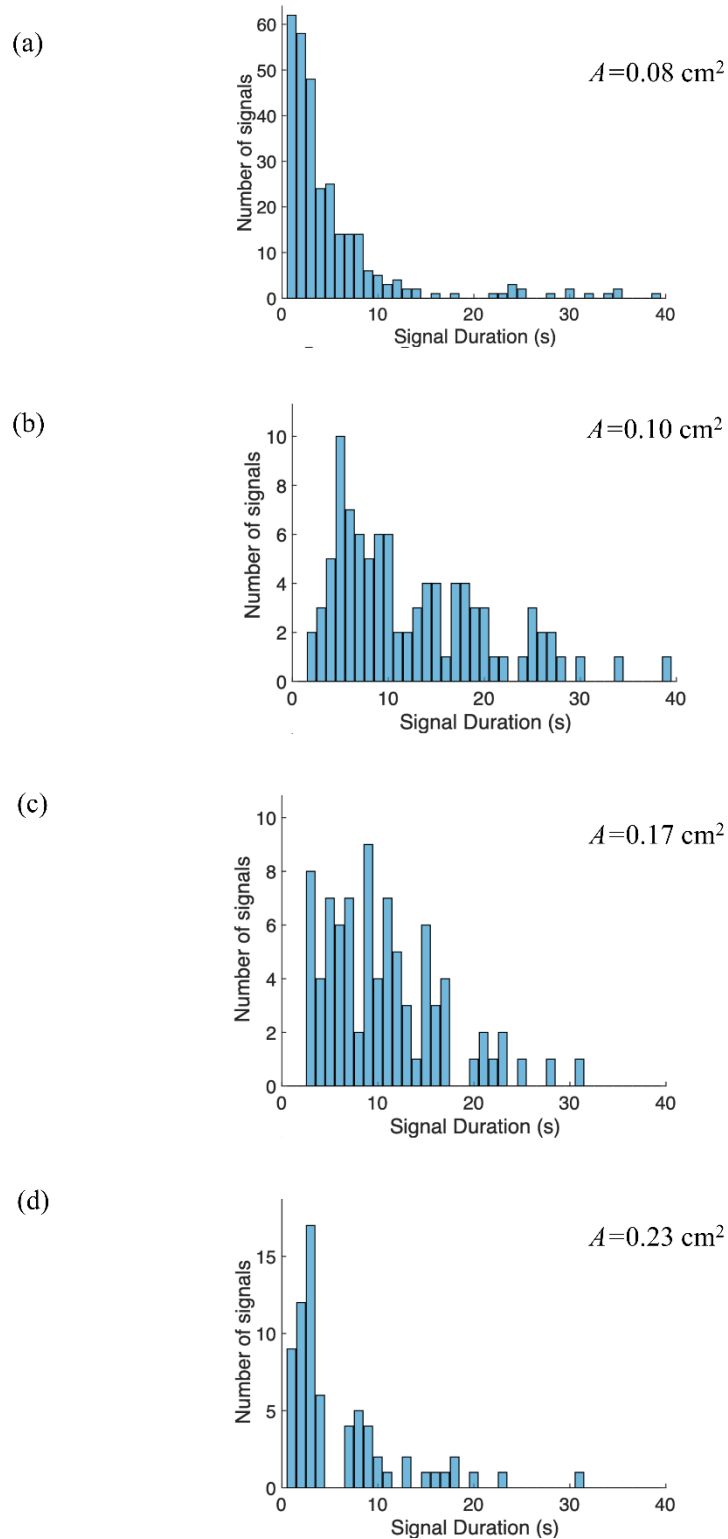


**Figure 5. 8** Comparison of signal duration for round electrodes with different electrode areas. Electrode geometry is represented in Figure 5.3.

## 5. Extracellular Astrocyte Signals

---

### 5.6. Discussion and Conclusions

This chapter investigates the impact of electrode geometry and active area on the properties of bioelectrical signals recorded from astrocyte populations. Specifically, it examines how variations in electrode area and design influence the fast component of the signal duration. Two distinct electrode configurations were employed. The first design used a constant round geometry while the active area was systematically varied. In the second design, circular electrodes with different line widths were used, resulting in variations in electrode width and total area variations.

When analyzing discrete signals, a broad range of signal durations was observed, spanning from less than one second to up to 40 seconds. These signal durations were grouped into 1-second intervals, and the number of signals in each bin was recorded. It was found that electrodes with smaller areas exhibited a narrow signal duration distribution, peaking at 1 second, with a rapid decay. Signals longer than 10 seconds were rare for these smaller electrodes. The signal duration distribution broadened as the electrode area increased to 0.1 cm<sup>2</sup> and 0.17 cm<sup>2</sup>, with the peak shifting to 5 seconds. In principle larger electrodes can measure synchronized activity from larger clusters of cells. However, for the largest electrode ( $A = 0.23$  cm<sup>2</sup>), the distribution closely resembled that of the smallest electrode. The highest density of signals peaks at 3 seconds, slightly higher than the 1-second peak observed for the smallest electrode.

In summary, while larger electrodes can detect a broader distribution of signal durations, the differences are not substantial enough to draw definitive conclusions. This may be due to the influence of other factors, such as the way astrocyte populations organize. Astrocytes aggregate into clusters rather than forming continuous populations across the entire electrode surface. This clustering effect may have confounded the results, making the experiments less reliable. Additionally, in some experiments, the recordings were particularly noisy, making the detection of discrete signals challenging and contributing to the limited observations of clean discrete signals.

The investigation into electrode width did not provide evidence supporting the observation of travelling waves. The results were hampered by the difficulty in obtaining large confluent populations across the entire electrode geometry. This aggregation of the cells is likely hindered by the formation of travelling waves. As a result, our findings are inconclusive, and additional experiments will be necessary to clarify these observations.



# Chapter 6

## Chemical Stimulation of Astrocytes

This chapter examines the effects of various drugs on the bioelectrical behaviour of astrocyte cultures. Key steps include culture preparation, electrode placement, drug administration, medium exchange, and data analysis. Most results were consistent with the literature and in some experiments, a pronounced system response was observed following the medium exchange after drug administration.

## 6. Chemical Stimulation of Astrocytes

---

### 6.1. Introduction

It is crucial to demonstrate that we can intentionally disrupt the bioelectrical activity of astrocyte populations. One effective method to induce such changes is by exposing the cell culture to drugs known to interact with ion channels. If these changes in the bioelectrical activity can be recorded reproducibly, it contributes to validate our bioelectrical devices and methods.

This chapter presents the bioelectrical responses of confluent astrocyte cell populations to a variety of drugs. The selected drugs were chosen based on literature reports indicating their effects on ion channels. The drugs used include Ethylene Glycol Tetraacetic Acid (EGTA), caffeine, norepinephrine, dopamine, and calcium chloride. Additionally, the effects of pH changes in the cell culture medium were explored.

Changes in perfusion conditions, which involve replacing the spent cell culture medium with fresh medium, can dramatically alter cellular metabolism. For example, it has been shown in fibroblasts that increasing perfusion rates leads to higher nutrient consumption rates and increased cellular metabolism [65]. Therefore, changes in perfusion conditions are also expected to affect the bioelectrical activity of the cell population and were discussed in this chapter.

Following this introduction, which outlines the main purpose of exposing cell populations to drugs, the subsequent sections provide information about each administered drug, including their properties and expected effects on astrocyte activity. The experimental methods used for drug administration, the specific concentrations applied, and the experimental setup are also presented. In the results section, the effects of each drug on the astrocyte population are presented. The impact of the drugs on astrocyte population activity is presented both in the time and frequency domain. The results are discussed in detail in a separate section before the main conclusions are outlined.

### 6.2. Drug description

This section presents the drugs used and their possible effects on astrocytic cells. It will discuss each substance's mechanisms of action, their specific interactions with astrocytes and neurons, and their impact on cellular communication and brain function.

#### (a) EGTA

## 6. Chemical Stimulation of Astrocytes

---

EGTA, also known as egtazic acid, is a widely used calcium chelating agent in neuroscientific research due to its high specificity for calcium ions compared to other cations. This compound can bind strongly to free calcium ions within the cell, forming stable complexes that prevent these ions from interacting with other molecules [66].

Calcium chelators like EGTA reduce intracellular calcium levels by binding free calcium ions [67]. This directly lowers the activation of calcium-dependent channels and pathways, reducing cellular excitability. In astrocytes, this decrease in calcium availability suppresses signalling and leads to lower overall activity. Thus, the primary effect of EGTA is a reduction in cellular activity due to the reduced intracellular calcium concentration.

### (b) Caffeine

Caffeine (1, 3, 7-trimethylxanthine) is a naturally occurring alkaloid found in different ways in the daily lives of all people [68]. Caffeine significantly influences neural processes, especially by blocking adenosine receptors, including subtypes A1 and A2A, which are expressed in both astrocytes and neurons. A1 receptors inhibit neuronal activity, conserving energy, while A2A receptors promote glucose uptake and play a role in regulating energy metabolism. Blocking these receptors by caffeine leads to greater neuronal excitability, increasing cellular activity, which can alter neurotransmitter release and synaptic communication [69].

Caffeine also plays a role in modulating intracellular calcium mobilization and influencing the activity of synaptic receptors and channels, leading to plastic changes in synaptic transmission efficiency and synaptic morphology. By activating ryanodine receptors, caffeine lowers the threshold for intracellular calcium release, thereby enhancing cell signalling [70].

### (c) Calcium chloride

Calcium chloride,  $\text{CaCl}_2$ , is an ionic halide. When administered to astrocytes, it increases the concentration of calcium ions ( $\text{Ca}^{2+}$ ) in the intracellular medium due to its dissociation in a culture medium. The literature states that this substance influences homeostasis and even regulates astrocyte volume [71].

## 6. Chemical Stimulation of Astrocytes

---

One of the main communication pathways and multicellular responses in astrocytes involves propagating calcium waves [72]. Communication between astrocytes relies on the presence of calcium: a local increase in intracellular calcium can trigger the propagation of a calcium wave to neighbouring cells.

The presence of calcium is crucial for this communication once a local increase in calcium levels within an astrocyte, often triggered by inositol trisphosphate receptor (IP3) receptor activation, can propagate as a calcium wave [73]. The higher the calcium concentration within an astrocyte, the more likely communication through calcium waves is to occur.

### **(d) Norepinephrine**

Norepinephrine is a neurotransmitter. There are studies indicating that norepinephrine can alter the response of astrocytes to nearby neural activity, increasing both the magnitude of the response and the proportion of responding astrocytes.

Norepinephrine induces widespread calcium responses in astrocytes, effect that can be disrupted by gliotoxins and the conditional suppression of exocytosis in astrocytes and can be blocked by antagonists of the gliotransmitter ATP [74].

Norepinephrine is a key factor in the stress response. It activates neurons in the hypothalamus that release corticotropin-releasing hormone (CRH). This activation involves a signalling process in the dendrites, which, in turn, involves astrocytes [75].

In the literature it has been shown that norepinephrine significantly influences astrocytes by inducing large, dose-dependent  $\text{Ca}^{2+}$  responses [76]. Based on this information, a positive influence on the activity and communication of the astrocyte culture is expected, as well as the influence of the concentration of norepinephrine used.

### **(e) Dopamine**

Dopamine is a key neurotransmitter in the mammalian brain and cultured astrocytes have been found to exhibit rapid dopamine uptake [77].

Astrocytes possess two distinct types of dopamine receptors: D1 receptors, which have an excitatory function, and D2 receptors, which serve an inhibitory role. Upon activation of D1 receptors, there is a subsequent increase in the intracellular calcium ions ( $\text{Ca}^{2+}$ ) concentration within the astrocytes. This rise in  $\text{Ca}^{2+}$  can then initiate the release

## 6. Chemical Stimulation of Astrocytes

---

of gliotransmitters, thereby influencing synaptic communication and neuronal activity [78].

The increase in  $\text{Ca}^{2+}$  modulates the excitability of astrocytes, increasing both intracellular and intercellular signalling and, consequently, affecting neuronal function and synaptic communication. However, the response of astrocytes to dopamine is not yet fully understood; evidence suggests that astrocytic responses may vary depending on the brain region [79].

### (f) Glutamate

Glutamate is the primary mediator of sensory information, motor coordination, emotions, and cognition, including memory formation and retrieval. Beyond its role in these processes, glutamate plays a crucial part in metabolic communication between neurons and astrocytes and is involved in cell proliferation in cortical astrocytes [80].

The glutamate–glutamine cycle is an essential process occurring in astrocytes, that regulates the synthesis and recycling of glutamate between neurons and astrocytes. This cycle is based on the discovery that the enzyme responsible for synthesizing glutamine from glutamate is expressed in astrocytes but not in neurons. This finding led to the understanding that glutamate released from neurons is transported into astrocytes, converted to glutamine, and subsequently returned to neurons. In neurons, glutamine is converted back to glutamate [81].

Excessive glutamate administration has been shown to disrupt communication between brain cells, particularly affecting astrocytes. This disruption can lead to impaired synaptic transmission, altered plasticity, and dysregulated intracellular signalling pathways [82]. However, in low concentrations, glutamate may increase astrocytic activity.

### (g) Acidified medium

Several studies in astrocytes reveal that pH affects excitability, neurotransmission, and responses to injury [83]. It has also been established that cultured mammalian astrocytes pH is sensitive to changes in membrane voltage [84].

When cells are exposed to an acidic medium, an abrupt drop in intracellular pH, (herein referred to as pHi) is expected immediately. The cells' response can be complex, and the pattern of pHi regulation in certain types of cells tends to be unique. This response

## 6. Chemical Stimulation of Astrocytes

---

to acidification may be a partial or complete recovery of  $pH_i$ , and rapid morphological changes in astrocytes are known to occur [85].

Astrocytic pH dysregulation is implicated in various diseases, making research particularly interesting. Astrocytic pH regulatory mechanisms could offer a promising therapeutic approach to modulating brain acid-base balance [86].

### 6.3. Experimental Methods

The electrical recording setup used in this chapter is the one described in Chapter 4, Experimental Methods. The cells were cultured and prepared for experimentation, as explained in Chapter 5. The sensing devices were electrodes purchased by applied Biophysics, also described in Chapter 4. The sensing electrode has an active area of  $0,49 \text{ cm}^2$ .

The astrocyte populations were chemically stimulated using the following procedure. Cell-culture medium solutions containing precise drug concentrations were prepared in advance. After recording the bioelectrical baseline, electrical measurements were temporarily paused, and the cell culture medium was completely removed from the device. The medium was replaced with a fresh solution containing the defined drug concentration, and electrical measurements resumed. Exposure times ranged from 30 to 60 minutes (See Table 6.1). Upon completion of the exposure period, electrical measurements were paused once more, and the medium was replaced with a fresh cell culture medium without the drug.

## 6. Chemical Stimulation of Astrocytes

---

**Table 6. 1** Drugs used in this study. The concentration and exposure times are outlined.

Drug	Concentration	Exposure Time (minutes)
EGTA	100 $\mu$ M	45
	500 $\mu$ M	50
Caffeine	2.5 mM	60
Calcium Chloride	5 mM	60
	10 mM	50
Norepinephrine	5 mM	30
Dopamine	10 mM	30
	2.5 mM	30
Glutamate	2.5 mM	30
	5 mM	60
Acidified Medium	pH= 6.2	45
	pH= 5.4	45

### 6.4 Results and analysis

This section details the responses of astrocyte populations to various drugs. Initially, the cell population activity is recorded to establish a clear baseline. Subsequently, the bioelectrical activity is monitored during drug exposure and after the drug-containing medium is replaced with a fresh medium.

Multiple consecutive drug exposure experiments are often conducted, with increasing drug concentrations.

#### (a) Response to EGTA

The effects of EGTA at two different concentrations, 100  $\mu$ M and 500  $\mu$ M, were investigated. The results are presented in Figures 6.1, 6.2, and 6.3. Bioelectrical recordings are shown in the time and frequency domains.

## 6. Chemical Stimulation of Astrocytes

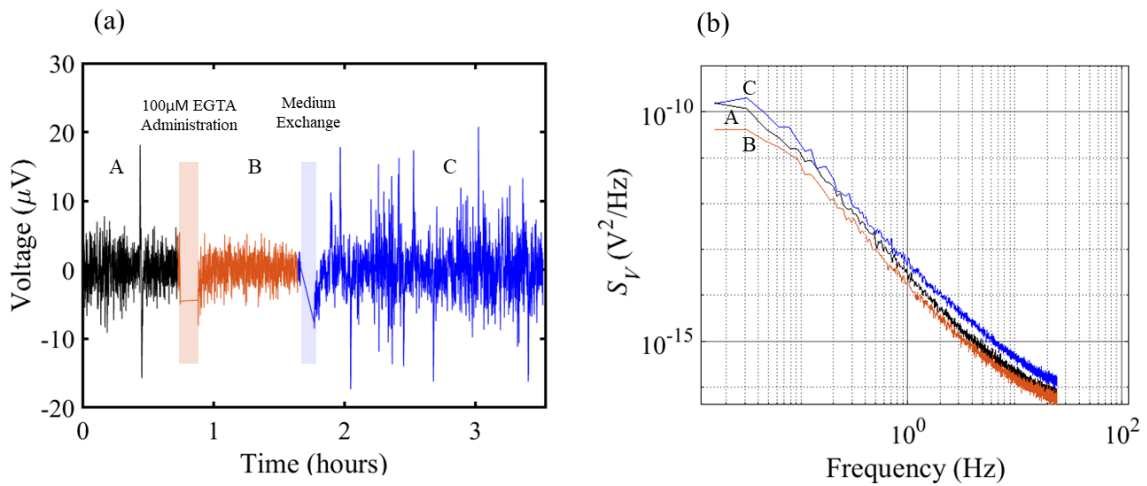


**Figure 6. 1 (a)** Recordings of bioelectrical activity before, during and after administration of EGTA at a concentration of 100  $\mu\text{M}$  **(b)** Power spectral density of the voltage noise,  $S_V$ , as a function of frequency. (A) Before exposure (B) During exposure and (C) Drug wash with replacement with a fresh cell-culture medium.

Upon EGTA exposure, the average noise level decreases as expected, since EGTA disrupts cell-cell connections and inhibits communication with neighbouring cells. Consequently, the activity remains low, nearing the baseline electrode noise level. However, a pronounced increase in bioelectrical activity is observed after the medium is replaced with fresh culture medium (without EGTA).

While the cells exhibited activity in the fresh medium, a second administration of EGTA at a higher concentration was carried out. The results of this experiment are presented in Fig. 6.2. Contrary to expectations, the second administration of EGTA does not have a clearly visible effect on bioelectrical activity.



## 6. Chemical Stimulation of Astrocytes

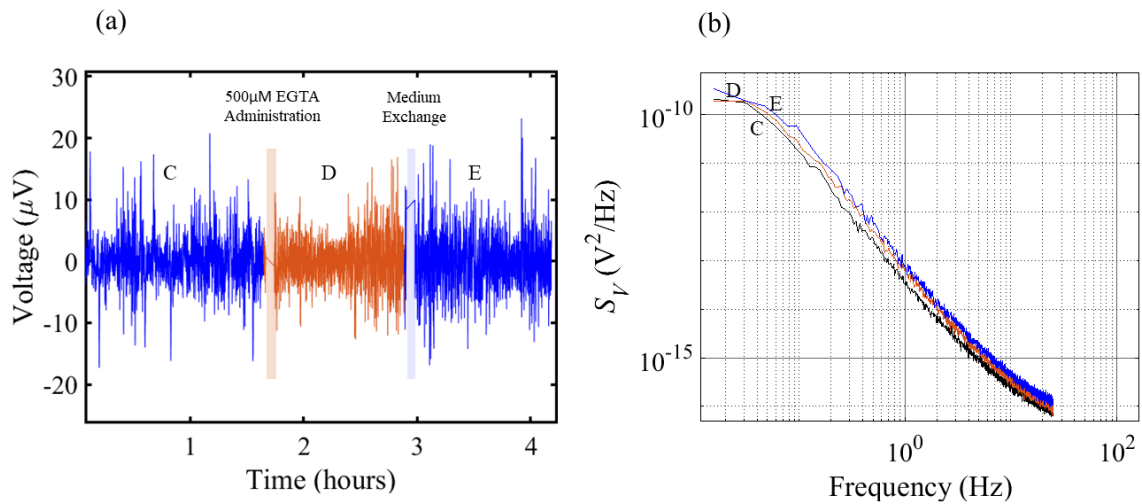


**Figure 6. 2 (a)** Recordings of bioelectrical activity before, during and after administration of EGTA at a concentration of 500  $\mu\text{M}$  (b) Power spectral density of the voltage noise,  $S_V$ , as a function of frequency. (C) Before exposure (D) During exposure and (E) Drug wash with replacement with a fresh cell-culture medium.

Figure 6.3 presents an overview of the effect on the bioelectrical activity of an astrocyte population following two consecutive EGTA administrations at increasing concentrations. Interestingly, the second administration did not completely silence cellular activity, though the reasons for this remain unclear.

## 6. Chemical Stimulation of Astrocytes

---

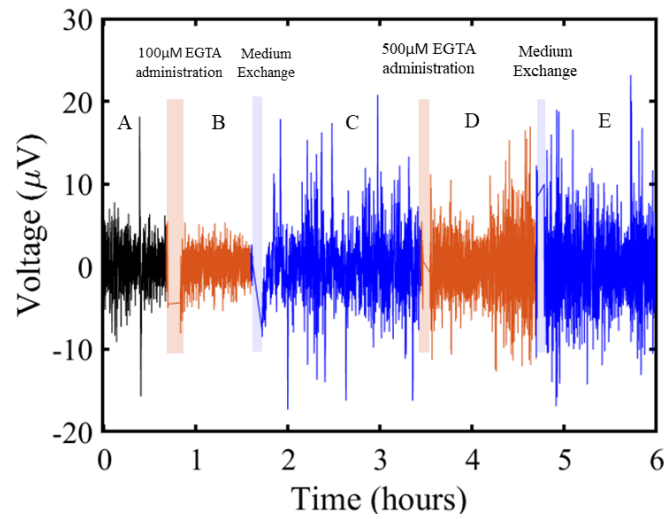


**Figure 6. 3** Bioelectrical response of an astrocyte population to two consecutive EGTA administrations at increasing concentrations.

### (b) Response to Caffeine

In this experiment, astrocytes were exposed to caffeine at a concentration of 2.5 mM. According to the literature, an increase in cellular activity was anticipated; however, this was not reflected in our bioelectrical recordings. Figure 6.4 illustrates the response to caffeine administration, with the bioelectrical data presented in both time and frequency domains. During caffeine exposure, the activity remained nearly unchanged. However, following the replacement of the cell culture medium with fresh medium, a significant increase in the average amplitude of the oscillations was observed.

## 6. Chemical Stimulation of Astrocytes

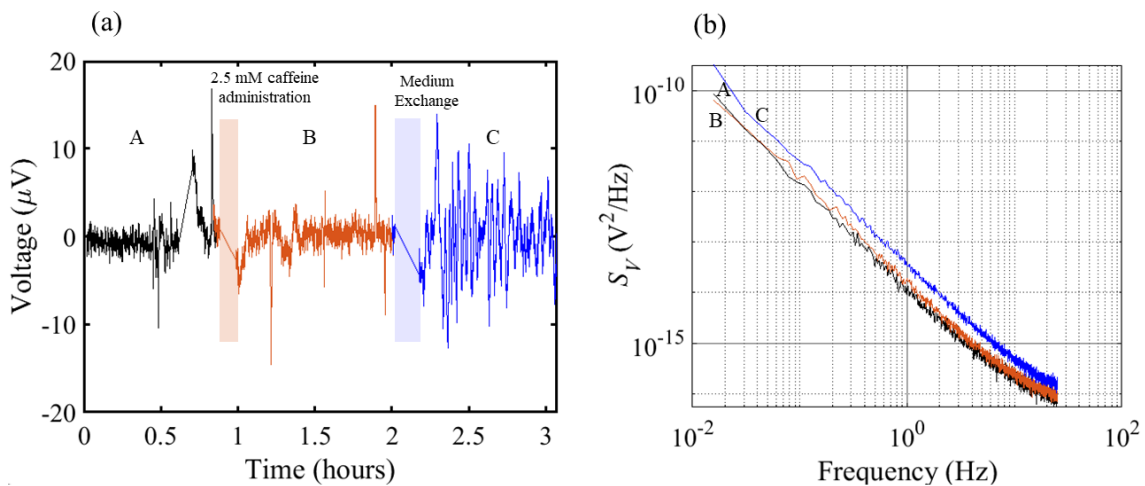


**Figure 6. 4 (a)** Recordings of bioelectrical activity before, during and after administration of caffeine at a concentration of 2.5 mM **(b)** Power spectral density of the voltage noise,  $S_V$ , as a function of frequency. (A) Before exposure (B) During exposure and (C) Drug wash with replacement with a fresh cell-culture medium.

### (c) Response to Calcium Chloride

The effects of calcium chloride ( $\text{CaCl}_2$ ) administration on the bioelectrical activity of astrocyte populations were evaluated at two concentrations: 5 mM and 10 mM. The anticipated outcome was an increase in activity, with higher concentrations expected to produce a more pronounced effect. Figures 6.5, 6.6, and 6.7 present the results in both time and frequency domains.

The administration of  $\text{CaCl}_2$  had minimal impact on astrocyte bioelectrical activity. In the frequency domain, the separation of the two curves is caused by the presence of two discrete signals. Sporadic signals were also recorded before  $\text{CaCl}_2$  exposure, making it difficult to attribute these signals to  $\text{CaCl}_2$  conclusively. After one hour of exposure, the cell culture medium was replaced with a fresh medium without  $\text{CaCl}_2$ .

Again, upon washing with a fresh cell culture medium, a significant increase in the astrocyte bioelectrical activity is recorded (see Fig. 6.5).

## 6. Chemical Stimulation of Astrocytes

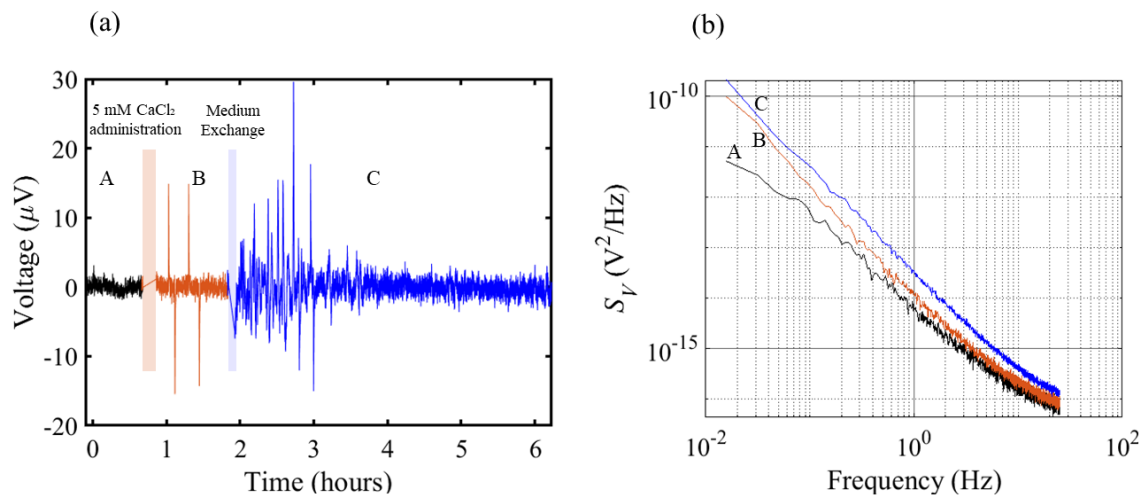


**Figure 6. 5 (a)** Recordings of astrocyte bioelectrical activity before, during and after administration of CaCl<sub>2</sub> at a concentration of 5 mM **(b)** Power spectral density of the voltage noise,  $S_V$ , as a function of frequency. (A) Before exposure (B) During exposure and (C) Drug wash with replacement with a fresh cell-culture medium.

A second consecutive administration causes a slight increase in the bioelectrical activity, which remains high even after washing of the drug with a fresh cell culture medium.

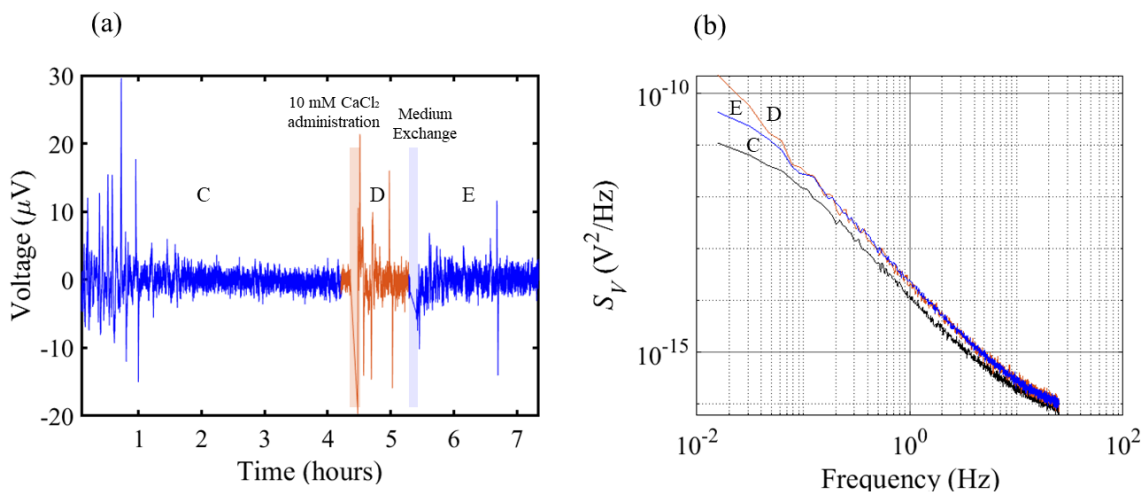


**Figure 6. 6 (a)** Recordings of bioelectrical activity before, during and after administration of CaCl<sub>2</sub> at a concentration of 10 mM **(b)** Power spectral density of the voltage noise,  $S_V$ , as a function of frequency. (A) Before exposure (B) During exposure and (C) Drug wash with replacement with a fresh cell-culture medium.

## 6. Chemical Stimulation of Astrocytes

Figure 6.7 provides an overview of two consecutive  $\text{CaCl}_2$  administrations on the bioelectrical activity of astrocytes.

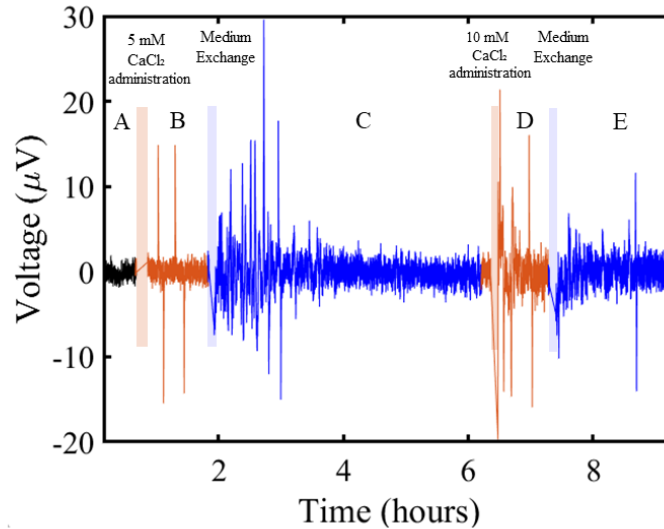


**Figure 6. 7** The effect of  $\text{CaCl}_2$  administration on the astrocyte activity. Two consecutive administrations with increasing  $\text{CaCl}_2$  concentrations were carried out.

### (d) Response to Norepinephrine

The effects of norepinephrine exposure on astrocyte activity using the concentration of 5 mM are presented in Figure 6.8. The data is presented both in time as well as in the frequency domains.

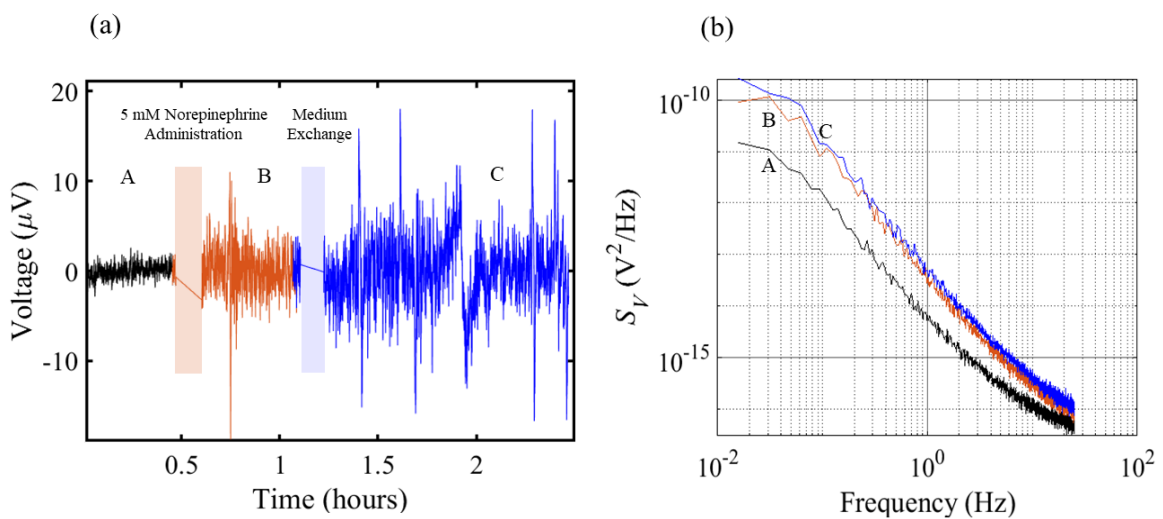


**Figure 6. 8 (a)** Recordings of bioelectrical activity before, during and after administration of norepinephrine at a concentration of 5 mM **(b)** Power spectral density of the voltage

## 6. Chemical Stimulation of Astrocytes

noise,  $S_V$ , as a function of frequency. (A) Before exposure (B) During exposure and (C) Drug wash with replacement with a fresh cell-culture medium.

Norepinephrine induces strong astrocyte bioelectrical activity (as expected), which remains high throughout the drug exposure period. Even upon washing, the activity remains high. This behaviour is represented in Fig. 6.8.

### (e) Response to Dopamine

The study examined the effects of dopamine administration at concentrations of 2.5 mM and 10 mM on astrocytic activity, as illustrated in Figure 6.9. The astrocyte bioelectrical activity increases as expected. Upon wash the activity slowly decreases with time

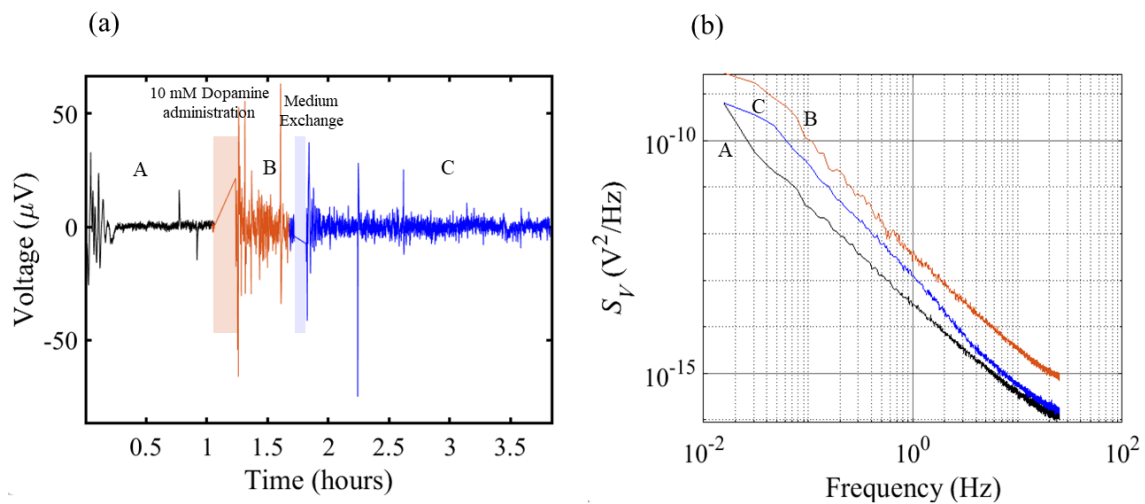


**Figure 6. 9** (a) Recordings of bioelectrical activity before, during and after administration of dopamine at a concentration of 10 mM (b) Power spectral density of the voltage noise,  $S_V$ , as a function of frequency. (A) Before exposure (B) During exposure and (C) Drug wash with replacement with a fresh cell-culture medium.

A second consecutive administration of dopamine did not produce any noticeable effects on the bioelectrical activity. The results of both consecutive administrations are summarized in Figure 6.11.

## 6. Chemical Stimulation of Astrocytes

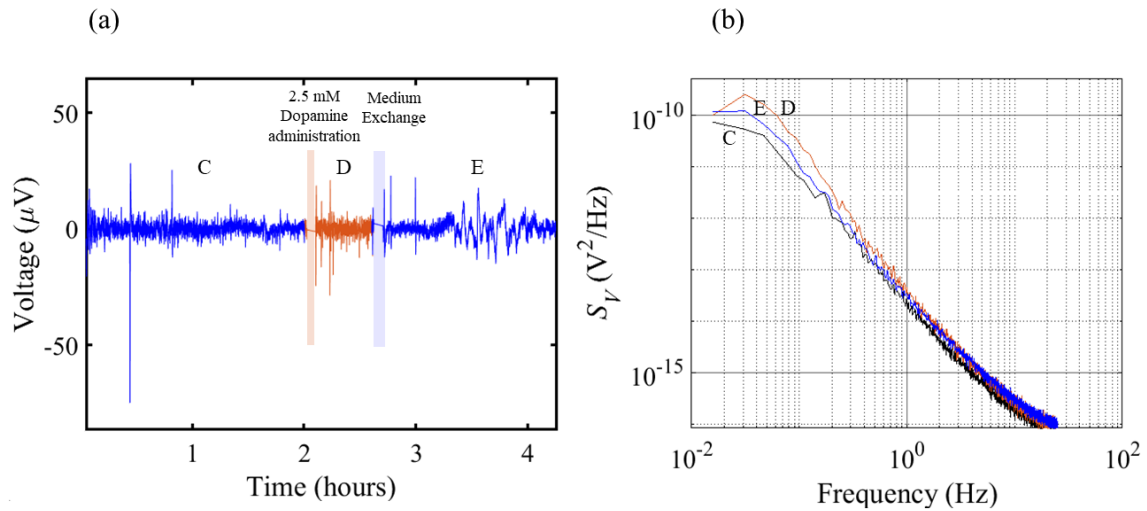


**Figure 6. 10** (a) Recordings of bioelectrical activity before, during and after administration of dopamine at a concentration of 2.5 mM (b) Power spectral density of the voltage noise,  $S_V$ , as a function of frequency. (A) Before exposure (B) During exposure and (C) Drug wash with replacement with a fresh cell-culture medium

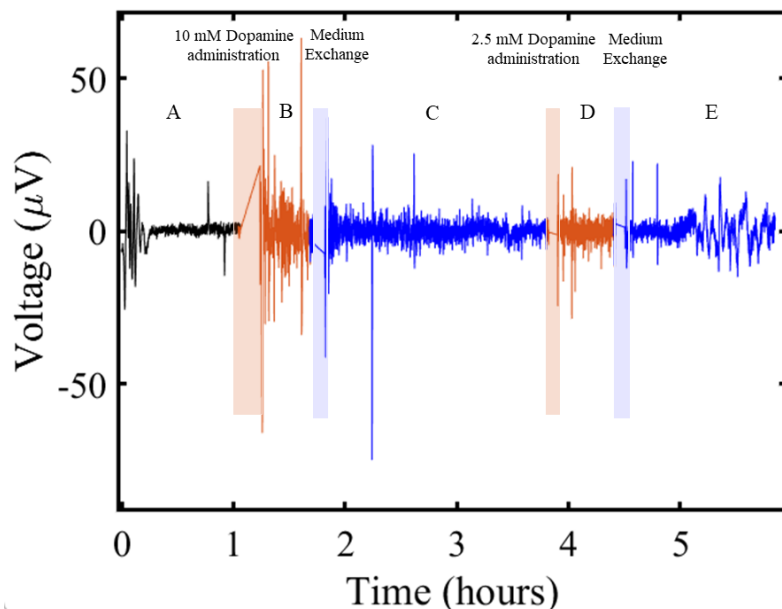


**Figure 6. 11** The astrocyte bioelectrical activity response to two consecutive dopamine exposures with increasing concentration

## 6. Chemical Stimulation of Astrocytes

### (f) Response to Glutamate

The effects of glutamate administered at concentrations of 2.5 mM and 5 mM on astrocytic activity were also investigated, with results presented in Figures 6.12 and 6.13. As anticipated, an increase in astrocytic activity was observed. However, these results are not entirely conclusive, as the electrophysiological traces show discrete bioelectrical signals that complicate the interpretation of the activity. These signals may appear spontaneously. To reach a conclusion, these experiments must be repeated several times, and a statistical analysis must be carried out to ensure that the results are reproducible.

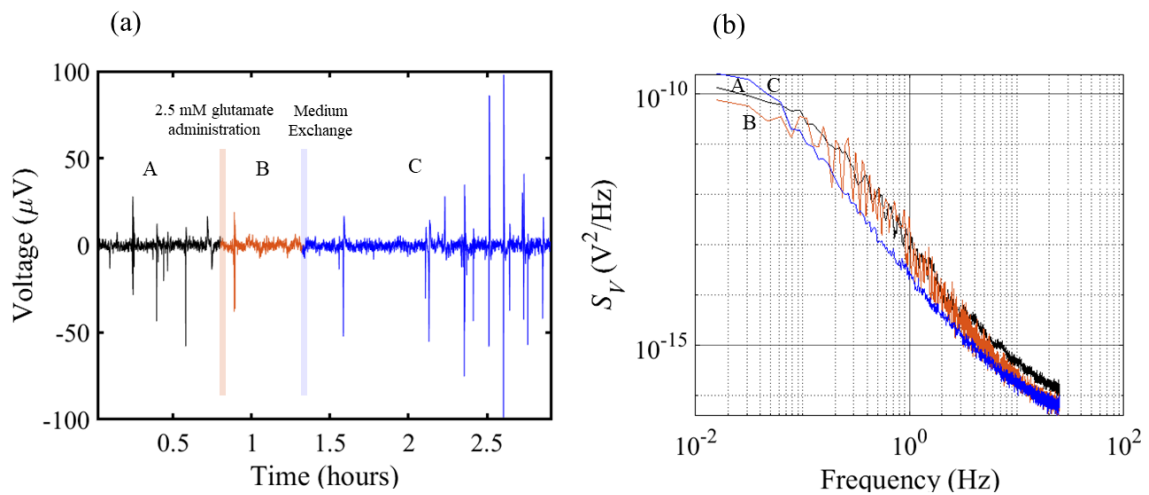


**Figure 6. 12 (a)** Recordings of bioelectrical activity before, during and after administration of glutamate at a concentration of 2.5 mM **(b)** Power spectral density of the voltage noise,  $S_V$ , as a function of frequency. (A) Before exposure (B) During exposure and (C) Drug wash with replacement with a fresh cell-culture medium.



## 6. Chemical Stimulation of Astrocytes

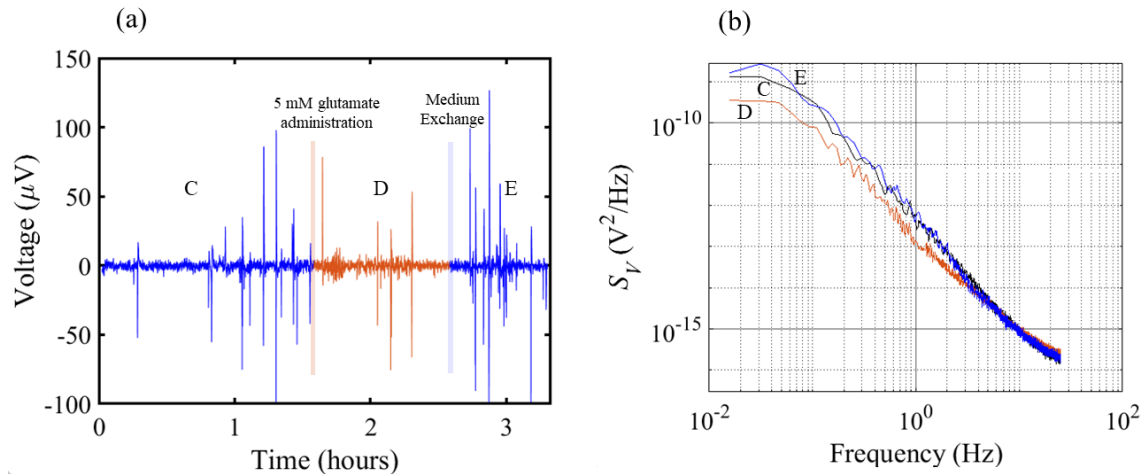


**Figure 6.13** (a) Recordings of bioelectrical activity before, during and after administration of glutamate at a concentration of 5 mM (b) Power spectral density of the voltage noise,  $S_V$ , as a function of frequency. (A) Before exposure (B) During exposure and (C) Drug wash with replacement with a fresh cell-culture medium

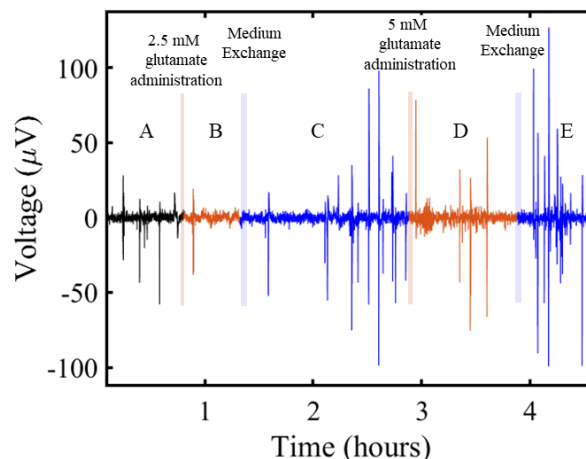


**Figure 6.14** The astrocyte response to two consecutive glutamate exposures with increasing concentration.

In the initial glutamate administration, depicted in Figure 6.12, no significant changes in activity were observed during drug exposure, aside from disturbances in the noise level. However, a notable increase in activity was detected approximately 2 hours later, following the medium change.

During the second glutamate administration, shown in Figure 6.13, activity remained elevated, with no disturbances in noise across the different phases (Figure 6.12).

## 6. Chemical Stimulation of Astrocytes

This sustained increase in activity is clearly illustrated in Figure 6.14, where it remains significantly higher compared to the baseline from Phase C onwards.

### (g) Response to Acidified Medium

We studied the effects of exposing astrocytes to culture medium with pH levels of 6.2 and 5.4. The results are depicted in Figs. 6.16, 6.16, and 6.17. For comparison, the resting pHi in cultured astrocytes is reported to be  $6.82 \pm 0.06$  [19].

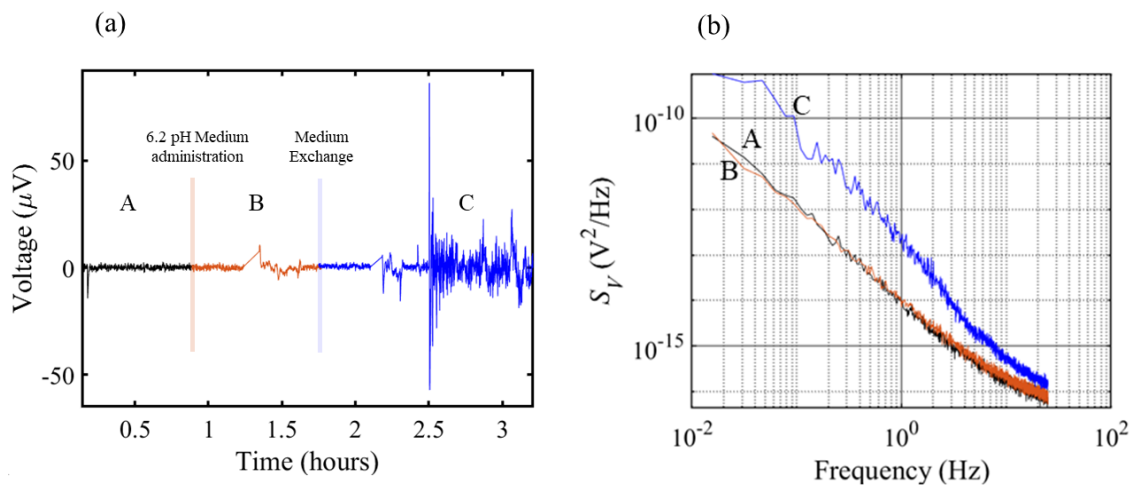


**Figure 6. 15 (a)** Recordings of bioelectrical activity before, during and after acidic medium administration (pH=6.2) **(b)** Power spectral density of the voltage noise,  $S_V$ , as a function of frequency. (A) Before exposure (B) During exposure and (C) Drug wash with replacement with a fresh cell-culture medium.

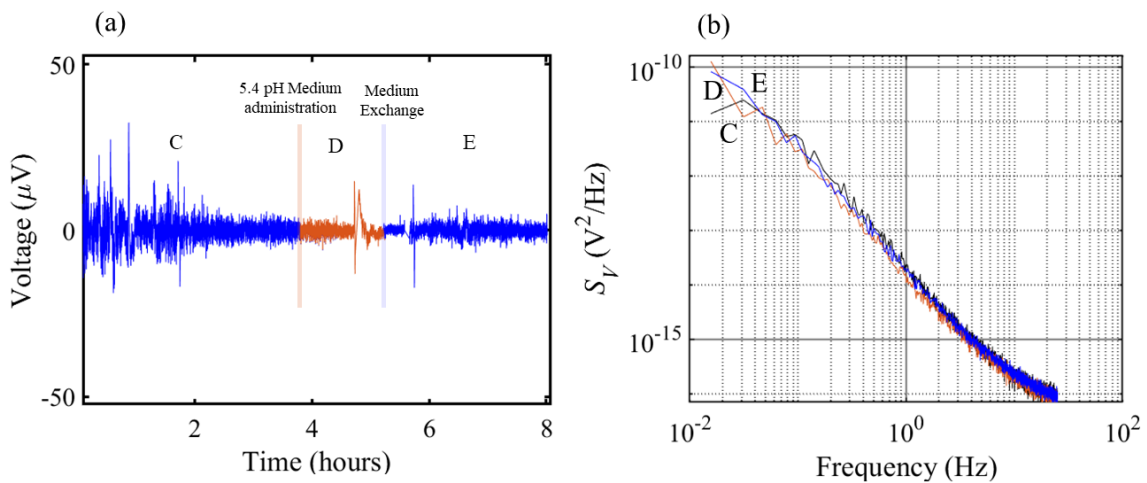


**Figure 6. 16 (a)** Recordings of bioelectrical activity before, during and after acidic medium administration (pH=5.4) **(b)** Power spectral density of the voltage noise,  $S_V$ , as a function

## 6. Chemical Stimulation of Astrocytes

---

of frequency.(C) Before exposure (D) During exposure and (E) Drug wash with replacement with a fresh cell-culture medium.

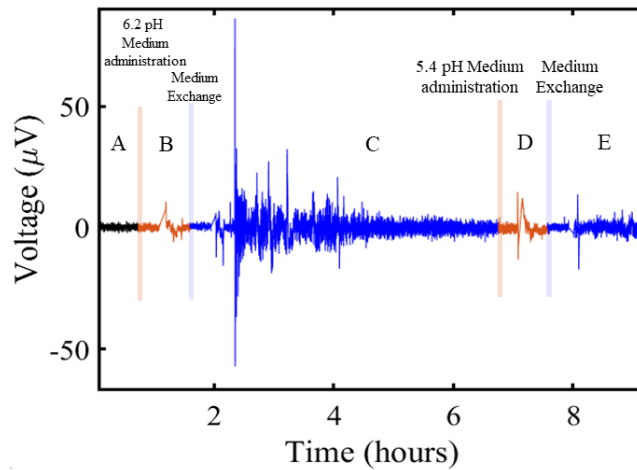


**Figure 6. 17** The response of astrocytes to two consecutive pH changes.

Following the administration of the acidic medium (pH = 6.2) and the subsequent medium exchange, a significant increase in activity is observed, as shown in Figure 6.15. In contrast, the subsequent acidification of the medium (pH = 5.4) did not noticeably affect the bioelectrical activity of the astrocytes (Figure 6.16).

In Figure 6.15, the increase in noise during Phase C is prominent and persists through the subsequent phases, as illustrated in Figure 6.16. Figure 6.17 demonstrates a surge in activity during Phase C, which gradually diminishes over several hours.

### 6.4. Discussion

The conclusions from the drug exposure experiments are summarised in Table 6.2.

## 6. Chemical Stimulation of Astrocytes

---

**Table 6. 2** Main conclusions of each drug

<b>Drug</b>	<b>Main observations</b>
EGTA	Initial decrease in activity during exposure. Increase in noise, influenced by the medium exchange rather than the administration of the drug
Caffeine	Notable influence in astrocytic activity, which becomes even more pronounced after the medium exchange.
Calcium Chloride	Increased astrocytic activity, different response to the two concentrations of the drug used.
Norepinephrine	Great influence in astrocytic activity, which becomes more pronounced after the medium exchange.
Dopamine	Increase in astrocytic activity after administration of the drug at only its highest concentration.
Glutamate	Increase in activity not immediately after the medium change
Acidified Medium	Increase in astrocytic activity after the change of medium relative to the administration of the less acidic medium

### 6.5. Conclusions

All the drugs tested in this study elicited responses in astrocytic activity. It was also observed that drug concentrations could have a significant influence on astrocytic activity, as expected. These variables underscore the complexity and variability inherent in astrocyte responses.

One key aspect observed in our investigation is the critical role of medium exchange in modulating astrocytic activity. Studies found that medium exchange can provide fresh nutrients and remove toxins, creating a more favourable environment for cellular activity [1]. This context is particularly relevant to our research with astrocytes, where in some experiments, we observed that these cells became more metabolically active when the medium was changed compared to when drugs were administered. This suggests that similar to fibroblastic cells, medium exchange is crucial in optimizing culture conditions to enhance cellular activity.

## 6. Chemical Stimulation of Astrocytes

---

The observed alterations in astrocytic behaviour following medium exchange are likely linked to the cells' intrinsic drive to maintain homeostasis and return to their initial state of equilibrium. Astrocytes have a well-documented capacity to modulate their activity in response to external stimuli, reflecting their essential role in maintaining the balance of the extracellular environment within the central nervous system. This dynamic responsiveness highlights the critical function of astrocytes in neural health.

One of the objectives was to determine whether the techniques used for measuring bioelectricity were responsive to stimuli. In conclusion, our findings indicate that this approach is effective in visualizing the effects of chemical stimulation on cell activity. The detection of changes in bioelectrical activity upon chemical exposure is an important validation step of our methodology and experimental set-up.

To gain a more detailed understanding of the effects of drug administration on astrocytic cultures, techniques such as calcium imaging, patch-clamp electrophysiology, and advanced imaging methods may provide greater precision.

# **Chapter 7**

## **Conclusions and future work**

This chapter outlines and discusses the major findings of this dissertation. It also presents some of the questions raised during this research, together with suggestions for experiments to elucidate them. Finally, it discusses how the methodology developed in this project can be applied in various areas.

## 7. Conclusions and future work

### 7.1. Main topics studied

This study investigates the bioelectrical signals recorded from astrocyte populations. Spontaneous activity was captured using extracellular electrodes and electrical low-noise recording techniques. To understand the nature of electrical oscillations generated by interconnected astrocytes.

Three key experiments were conducted in this study. The first study evaluated the dependence of the impedance on the cell culture medium composition and the long-term stability of the impedance parameters. The second experiment was designed to answer a critical question: Does electrode area and electrode geometry affect the properties of the recorded signals, specifically their duration and power? Finally, the third experiment evaluates how populations of astrocytes react to chemical stimulation. Populations of astrocytes were chemically stimulated, and the cell population's reaction to the presence of drugs was monitored by recording the bioelectrical fluctuations generated by the cell population. Below, there is a brief summary of these experiments and the major conclusions.

### 7.2. Conclusions

#### **(a) Long-term stability of the electro/electrolyte impedance and the effect of electrolyte composition on the capacitance and resistance parameters.**

The impedance of the EDL is not constant and varies over time, a factor that must be considered when performing long-term experiments. Both the electrode and the electrolyte play a role in influencing the impedance of the system. Research carried out in this dissertation explored how electrolyte composition impacts this variation over time, revealing that the electrolyte composition affects both the capacitance and resistance of the system.

Comparative studies of different media have shown that the chemical components of the electrolyte differentially influence the elements of the EDL's equivalent circuit. Salts, for instance, primarily affect the circuit's resistive component, reducing resistance, while sugars are more closely tied to the capacitive component. In contrast, proteins in culture media have little to no significant impact on the electrode-electrolyte impedance.

## 7. Conclusions and future work

### **(b) The role of the electrode in shaping the distribution of bioelectrical signals**

The role of the electrode in shaping the distribution of bioelectrical signals has been a long-standing problem. This can be summarized in two main questions:

- i) What is the ideal electrode area to record the bioelectrical activity of a particular cell population?
- ii) How does the geometry and area of the electrode influence the distribution of signal power, duration, and frequency in a long-term signal trace?

To provide an answer to these questions, we designed electrodes in different areas and geometries. The reason behind this strategy is that the discrete bioelectrical signals result from the synchronized activity of a cell cluster. Therefore, it is assumed that an ensemble of connected cells can synchronize their activity to generate a discrete signal. In theory, not all clusters have identical dimensions (the same number of cells), and probably, a cluster may grow or shrink in size during the synchronization process. This variability in the size of a synchronized cell cluster will cause a variability in signal power.

In addition, large-area electrodes are more likely to detect more clusters or large-size clusters. Small-area electrodes may limit the size of the cluster that can be detected. This limitation assumes that the synchronized cell clusters can be larger than the size of the sensing electrode.

In this study, we decided only to study well-defined signal shapes, such as biphasic signals. In addition, as a quantification parameter, we only measure the duration of the fast signal component of the biphasic signal. We assumed that the signal power is proportional to the duration of the fast component. Our results show that large-area electrodes may exhibit a broader distribution in signal durations than small-area electrodes. However, the results were not conclusive. We attribute this to the difficulty of obtaining well-spread and connecting cell populations across the entire electrode. Populations of astrocytes like to aggregate in clusters. This effect may mask the effect of varying the electrode area.

In addition to varying the active areas, we also designed circular electrodes with different widths. Assuming that signals are travelling oscillations when they cross electrodes with different widths, they should give rise to voltage signals with a duration proportional to the width of the electrodes. The signal duration should equal the product of the wave speed times the width of the electrode crossed by the wave. The findings were inconclusive because of the small number of signals recorded. Furthermore, in the same



## 7. Conclusions and future work

experiments, the confluent monolayer was not reached. A non-confluent cell monolayer cannot support traveling waves.

### **(c) Effects of the Chemical stimulation of astrocyte populations**

Chemical stimulation was intended to disrupt cellular activity and observe the resulting changes in bioelectrical signals. The hypothesis was that drugs known to interact with ion channels would significantly alter cell behaviour and, consequently, extracellular electrical oscillations. However, contrary to expectations, bioelectrical activity remained relatively stable, often becoming quieter immediately after drug exposure. Interestingly, bioelectrical activity surged above normal levels once the drug-laden medium was replaced with a fresh culture medium.

We propose the following explanation for this unexpected behaviour: under stress, cells may reduce or halt ion exchange with the extracellular medium, likely as a protective response to the toxic nature of the drug-laden medium. This mechanism allows cells to minimise harmful interactions with the surrounding environment. Once the drug is removed, the cells resume normal functioning (homeostasis) and restore ion exchanges, which may lead to a temporary spike in bioelectrical signal intensity. This phenomenon highlights the importance of homeostasis in understanding astrocyte behaviour.

While speculative, this explanation offers valuable insights into how pharmacological drugs interact with living cells. If cells possess a defence mechanism that involves shutting down membrane channels in response to high drug concentrations, this could have significant implications for clinical drug trials. Excessive doses may not yield the desired effects, as cells might actively reduce their responsiveness to protect themselves.

### **7.3. Further work**

The analysis of the findings and the resulting conclusions indicate the need for additional experiments to advance this research further. The proposed next steps for future work are outlined below.

## 7. Conclusions and future work

### **(a) Data analysis of the signal properties**

The distribution of the signal parameters should be carried out not in signal duration but in signal power. The signal power should be directly related to the number of cells synchronized. Therefore, all the electrode geometry and area analysis should be carried out using the signal power as a parameter. Furthermore, All the experiments should be carried out only when a complete confluence monolayer is established.

### **(b) Further research on the shape of the bioelectrical signals.**

Our model for detecting traveling waves using electrodes of varying widths assumes that the recorded voltage signals should be square-like in shape. In our analysis, we specifically focused on biphasic signals; however, these signals may not originate from traveling waves. As a result, our analysis may not fully apply to traveling wave phenomena. This brings up an intriguing question: what is the biological mechanism underlying the biphasic nature of these signals? Future experiments should be designed to investigate and provide insight into the origins of biphasic signals.

### **(c) Novel bioelectronic platform to evaluate the maximum drug concentrations.**

Contrary to our expectations, cell cultures do not respond immediately when exposed to high concentrations of chemicals. Instead, they suppress activity when the extracellular medium is perceived as toxic. This intriguing cellular behaviour could be leveraged as a tool in the pharmaceutical industry to assess optimal drug concentrations. To validate this hypothesis, a series of experiments should be conducted with progressively increasing drug concentrations.

### **(d) Bioelectrical activity of Astrocyte-neuron co-cultures.**

This dissertation initially aimed to measure the coculture of astrocytes and neurons. However, difficulties in obtaining confluent astrocyte monolayers prevented the timely analysis of the co-cultures for inclusion in this work. Future experiments that record and analyse the bioelectrical signals of cocultures should yield valuable insights into the role of astrocytes in neural networks.

## Bibliography

- [1] M. Berggren and A. Richter-Dahlfors, “Organic Bioelectronics,” *Advanced Materials*, vol. 19, pp. 3201–3213, 2007.
- [2] A. L. Hodgkin and A. F. Huxley, “A quantitative description of membrane current and its application to conduction and excitation in nerve,” *Bulletin of Mathematical Biology*, vol. 52, no. 1-2, pp. 25–71, 1990.
- [3] C. Fewtrell, “Ca<sup>2+</sup> Oscillations in Non-Excitable Cells,” *Annual Review of Physiology*, vol. 55, pp. 427–454, 1993.
- [4] E. Bindocci, I. Savtchouk, N. Liaudet, D. Becker, G. Carriero, and A. Volterra, “Three-dimensional Ca<sup>2+</sup> imaging advances understanding of astrocyte biology”, *Science*, vol. 356, no. 6339, pp. eaai8185, 2017.
- [5] M. Martin-Fernandez, S. Jamison, L. Robin, Z. Zhao, E. D. Martin, J. Aguilar, *et al.*, “Synapse-specific astrocyte gating of amygdala-related behavior”, *Nature Neuroscience*, vol. 20, no.11, pp. 1540–1548, 2017.
- [6] S. A. Liddelow, K. A. Guttenplan, L. E. Clarke, F. C. Bennett, C. J. Bohlen, L. Schirmer, *et al.*, “Neurotoxic reactive astrocytes are induced by activated microglia”, *Nature*, vol. 541, pp. 481–487, 2017.
- [7] W. S. Chung, N. J. Allen, and C. Eroglu, “Astrocytes Control Synapse Formation, Function, and Elimination”, *Cold Spring Harbor perspectives in biology*, vol. 7, no. 9, p. a020370, 2015.
- [8] N. J. Allen and C. Eroglu, “Cell Biology of Astrocyte-Synapse Interactions,” *Neuron*, vol. 96, no. 3, pp. 697–708, 2017.
- [9] F. Faramarzi, F. Azad, M. Amiri, and B. Linares-Barranco, “A Neuromorphic Digital Circuit for Neuronal Information Encoding Using Astrocytic Calcium Oscillations,” *Frontiers in Neuroscience*, vol. 13, p. 453882, 2019
- [10] M. E. Spira and A. Hai, “Multi-electrode array technologies for neuroscience and cardiology,” *Nature Nanotechnology*, vol. 8, no. 2, pp. 83–94, 2013.
- [11] V. Houades, N. Rouach, P. Ezan, F. Kirchhoff, A. Koulakoff, and C. Giaume, “Shapes of astrocyte networks in the juvenile brain,” *Neuron Glia Biology*, vol. 2, no. 1, p. 3, 2006.

## Bibliography

- [12] K. Matthias, F. Kirchhoff, G. Seifert, K. Hüttmann, M. Matyash, H. Kettenmann, and C. Steinhäuser, “Segregated expression of AMPA-type glutamate receptors and glutamate transporters defines distinct astrocyte populations in the mouse hippocampus,” *The Journal of Neuroscience*, vol. 23, no. 5, pp. 1750–1758, 2003.
- [13] T. Deemyad, J. Lüthi, and N. Spruston, “Astrocytes integrate and drive action potential firing in inhibitory subnetworks,” *Nat Commun*, vol. 9, p. 4336, 2018.
- [14] Scientifica, “Using cell-attached patch clamp to monitor neuronal activity,” 2020. Accessed: 2024-06-16.
- [15] L. Microsystems, “The patch clamp technique,” 2018. Accessed: 2024-06-30.
- [16] M. E. J. Obien, K. Deligkaris, T. Bullmann, D. J. Bakkum, and U. Frey, “Revealing neuronal function through microelectrode array recordings”, *Frontiers in Neuroscience*, vol. 8, p.423, 2015.
- [17] M. Ferguson, D. Sharma, D. Ross, and F. Zhao, “A Critical Review of Microelectrode Arrays and Strategies for Improving Neural Interfaces”, *Advanced healthcare materials*, vol. 8, no. 19, p. e1900558, 2019.
- [18] E. Wanke, F. Gullo, E. Dossi, G. Valenza, and A. Becchetti, “Neuron-glia cross talk revealed in reverberating networks by simultaneous extracellular recording of spikes and astrocytes’ glutamate transporter and K<sup>+</sup> currents,” *Journal of Neurophysiology*, vol. 116, pp. 2706–2719, 2016.
- [19] W. Fleischer, S. Theiss, J. Slotta, C. Holland, and A. Schnitzler, “High-frequency voltage oscillations in cultured astrocytes”, *Physiological Reports*, vol. 3, no. 5, p. e12400, 2015.
- [20] A. L. G. Mestre, P. M. C. Inácio, Y. Elamine, S. Asgarifar, A. S. Louren,co, M. L. S. Cristiano, and H. L. Gomes, “Extracellular electrophysiological measurements of cooperative signals in astrocytes populations,” *Frontiers in Neural Circuits*, vol. 11, p. 80, 2017.
- [21] A. L. G. Mestre, M. Cerquido, P. M. C. Inácio, S. Asgarifar, A. S. Louren,co, M. L. S. Cristiano, and H. L. Gomes, “Ultrasensitive gold micro-structured electrodes enabling the detection of extra-cellular long-lasting potentials in astrocytes populations,” *Scientific Reports*, vol. 7, no. 1, p. 14697, 2017.
- [22] P. R. F. Rocha, P. Schlett, L. Schneider, M. Dröge, V. Mailänder, H. L. Gomes, and D. M. de Leeuw, “Low frequency electric current noise in glioma cell populations,” *Journal of Materials Chemistry*, vol. 3, no. 25, pp. 5035–5039, 2015.

## Bibliography

- [23] M. Aroso, D. Castro, S. C. Silva, and P. Aguiar, "Bringing astrocytes into the spotlight of electrical brain stimulation," *bioRxiv*, 2024.
- [24] X. Wang, T. Takano, and M. Nedergaard, "Astrocytic Calcium Signaling: Mechanism and Implications for Functional Brain Imaging", *Dynamic Brain Imaging*, pp. 93–109, 2009.
- [25] B. S. Khakh and K. D. McCarthy, "Astrocyte Calcium Signaling: From Observations to Functions and the Challenges Therein", *Cold Spring Harbor Perspectives in Biology*, vol. 7, no. 4, p. a020404, 2015.
- [26] X. Liu, D. Lin, W. Becker, J. Niu, B. Yu, L. Liu, and J. Qu, "Fast fluorescence lifetime imaging techniques: A review on challenge and development", *Journal of Innovative Optical Health Sciences*, vol. 12, no. 1, p. 1930003, 2019.
- [27] S. E. B. Tyler, "Nature's Electric Potential: A Systematic Review of the Role of Bioelectricity in Wound Healing and Regenerative Processes in Animals, Humans, and Plants," *Frontiers in Physiology*, vol. 8, 2017.
- [28] H. D. Booth, W. D. Hirst, & R. Wade-Martins, "The role of astrocyte dysfunction in Parkinson's disease pathogenesis," *Trends in Neurosciences*, vol. 40, pp. 358-370, 2017
- [29] W. W. Chen, X. Zhang, & W. J. Huang, "Role of neuroinflammation in neurodegenerative diseases," *Molecular Medicine Reports*, vol. 13, pp. 3391-3396, 2009.
- [30] P. M. Rappold & K. Tieu, "Astrocytes and therapeutics for Parkinson's disease," *Neurotherapeutics: The Journal of the American Society for Experimental NeuroTherapeutics*, vol. 7, pp. 413-423, 2010.
- [31] A. M. Haidet-Phillips, M. E. Hester, C. J. Miranda, K. Meyer, L. Braun, A. Frakes, S. Song, S. Likhite, M. J. Murtha, K. D. Foust, M. Rao, A. Eagle, A. Kammesheidt, A. Christensen, J. R. Mendell, A. H. Burghes, and B. K. Kaspar, "Astrocytes from familial and sporadic ALS patients are toxic to motor neurons," *Nature Biotechnology*, vol. 29, no. 9, pp. 824–828, 2011.
- [32] M. Nagai, D. B. Re, T. Nagata, A. Chalazonitis, T. M. Jessell, H. Wichterle, & S. Przedborski, "Astrocytes expressing ALS-linked mutated SOD1 release factors selectively toxic to motor neurons," *Nature Neuroscience*, vol. 10, pp. 615-622, 2007

## Bibliography

- [33] R. van Passel, W. A. Schlooz, K. J. Lamers, W. A. Lemmens, and J. J. Rotteveel, "S100b protein, glia and Gilles de la Tourette syndrome," *European Journal of Paediatric Neurology*, vol. 5, no. 1, pp. 15–19, 2001.
- [34] C. de Leeuw, A. Goudriaan, A. B. Smit, D. Yu, C. A. Mathews, J. M. Scharf, T. S. A. I. C. for Genetics, M. H. Verheijen, and D. Posthuma, "Involvement of astrocyte metabolic coupling in Tourette syndrome pathogenesis," *European Journal of Human Genetics*, vol. 23, no. 11, pp. 1519–1522, 2015.
- [35] N. Ozkucur, H. H. Epperlein, and R. H. Funk, "Ion imaging during axolotl tail regeneration in vivo," *Developmental Dynamics*, vol. 239, pp. 2048–2057, 2010.
- [36] L. N. Vandenberg and M. Levin, "A unified model for endogenous bioelectric signaling in development, regeneration, and cancer: gap junctions, ion channels, and patterning," *Progress in Biophysics and Molecular Biology*, vol. 106, no. 2, pp. 137–185, 2012.
- [37] D. S. Adams and M. Levin, "Endogenous voltage gradients as mediators of cell-cell communication: strategies for investigating bioelectrical signals during pattern formation," *Cell Tissue Research*, vol. 352, pp. 95–122, 2013.
- [38] B. Song, "Nerve regeneration and wound healing are stimulated and directed by an endogenous electrical field in vivo," *Journal of Cell Science*, vol. 117, no. 20, pp. 4681–4690, 2004.
- [39] T. C. Südhof, "Neurotransmitter release: the last millisecond in the life of a synaptic vesicle," *Neuron*, vol. 80, no. 3, pp. 675–690, 2013.
- [40] A. K. McAllister, "Dynamic aspects of CNS synapse formation," *Annual Review of Neuroscience*, vol. 30, no. 1, pp. 425–450, 2007.
- [41] J. A. Noriega-Prieto and A. Araque, "Sensing and regulating synaptic activity by astrocytes at tripartite synapse," *Neurochemical Research*, vol. 46, pp. 2580–2585, 2021.
- [42] I. Farhy-Tselnicker and N. J. Allen, "Astrocytes, neurons, synapses: a tripartite view on cortical circuit development," *Neural Development*, vol. 13, p. 7, 2018.
- [43] R. Ventura and K. M. Harris, "Three-dimensional relationships between hippocampal synapses and astrocytes," *The Journal of Neuroscience*, vol. 19, no. 16, pp. 6897–6906, 1999.

## Bibliography

- [44] M. M. Halassa and P. G. Haydon, "Integrated brain circuits: astrocytic networks modulate neuronal activity and behavior," *Annual Review of Physiology*, vol. 72, pp. 335-355, 2010.
- [45] G. Dallérac, J. Zapata, and N. Rouach, "Versatile control of synaptic circuits by astrocytes: where, when and how?," *Nature Reviews Neuroscience*, vol. 19, pp. 729–743, 2018.
- [46] L. Adermark and D. M. Lovinger, "Electrophysiological properties and gap junction coupling of striatal astrocytes," *Neurochemistry International*, vol. 52, no. 7, pp. 1365–1372, 2008.
- [47] M. V. L. Bennett, L. C. Barrio, T. A. Bargiello, D. C. Spray, E. Hertzberg, and J. C. Sáez, "Gap junctions: New tools, new answers, new questions," *Neuron*, vol. 6, no. 3, pp. 305–320, 1991.
- [48] R. Dermietzel and D. C. Spray, "Gap junctions and electric synapses," in *Neuroscience in the 21st Century*, D. W. Pfaff, N. D. Volkow, and J. L. Rubenstein, Eds. Springer, Cham, 2022.
- [49] Yu, X., Nagai, J., and Khakh, B. S., "Improved tools to study astrocytes," *Nature Reviews Neuroscience*, vol. 21, pp. 121–138, 2020.
- [50] N. Uchida, T. Muraoka, "Self-assembling materials functionalizing bio-interfaces of phospholipid membranes and extracellular matrices," *Chemical Communications*, vol. 59, no. 75, pp. 9665-9678, 2023
- [51] E. H. Du Bois-Reymond, *Preliminary outline of an investigation into the so-called frog current and electromotor fish*. Berlin: G. Reimer, 1843.
- [52] C. Koch, M. Rapp, I. Segev, "A Brief History of Time (Constants)", *Cerebral Cortex*, vol. 6, no. 2, pp. 93-101, 1996.
- [53] Stony Brook University, "Cellular neurophysiology: Equivalent circuit of a cell", *NeuroText*, Retrieved Sep. 6, 2024, from [https://neurotext.library.stony-brook.edu/C3/C3\\_3/C3\\_3.html](https://neurotext.library.stony-brook.edu/C3/C3_3/C3_3.html).
- [54] G.T. Kovacs, "Enabling technologies for cultured neural networks" Stenger, D.A., McKenna, T.M., Eds.; Academic Press, 1994; ISBN 0126659702.
- [55] M.M.M Ahmed, and T. Imae, "Graphene-Based Nanolayers Toward Energy Storage Device"; *Elsevier*; pp. 353–389, 2017.
- [56] Randles, J.E.B. Kinetics of rapid electrode reactions. *Discuss. Faraday Soc.* 1952, 1, 11, doi:10.1039/df9470100011.

## Bibliography

- [57] W. Franks, I. Schenker, P. Schmutz, A. Hierlemann, "Impedance characterization and modeling of electrodes for biomedical applications", *IEEE Trans. Biomed. Eng.*, vol. 52, 1295–1302, 2005.
- [58] Applied Biophysics Inc., "8W1E PET 8-well array," Accessed: 2024-02-13. [Online]. Available: <https://applied-biophysics-inc.myshopify.com/products/8w1e-pet-8-well-array>
- [59] "Cell culture media, Dulbecco's Modified Eagle Medium", Accessed: 2024-01-30. [Online]. Available: <https://pt.vwr.com/store/product/12382443/null>
- [60] Thermo Fisher Scientific, "Sodium pyruvate solution (100 mM)," Accessed: 2024-09-13. [Online]. Available: <https://www.thermofisher.com/order/catalog/product/21127030?SID=srch-srp-21127030>
- [61] L. Leybaert, M. J. Sanderson, "Intercellular Ca<sup>2+</sup> Waves: Mechanisms and Function", *Physiological Reviews*, vol. 92, n° 3, pp. 1359–1392, 2012.
- [62] L. F. Jaffe, R. Créton, "On the Conservation of Calcium Wave Speeds", *Cell Calcium*, vol. 24, n° 1, pp. 1–8, 1998.
- [63] N. Kuga, T. Sasaki, Y. Takahara, N. Matsuki, Y. Ikegaya, "Large-Scale Calcium Waves Traveling through Astrocytic Networks In Vivo", *Journal of Neuroscience*, vol. 31, n° 7, pp. 2607–2614, 2011.
- [64] ATCC, "MCF 10A [ATCC CRL-2541™]," Accessed: 2024-03-03. [Online]. Available: <https://www.atcc.org/products/crl-2541>.
- [65] J. Caldwell, B. Locey, M. F. Clarke, S. G. Emerson, and B. O. Palsson, "Influence of medium exchange schedules on metabolic, growth, and GM-CSF secretion rates of genetically engineered NIH-3T3 cells," *Biotechnology Progress*, vol. 7, no. 1, pp. 1–8, 1991.
- [66] P. Schwartzkroin and C. Stafstrom, "Effects of EGTA on the calcium-activated afterhyperpolarization in hippocampal CA3 pyramidal cells," *Science*, vol. 210, no. 4474, pp. 1125–1126, 1980.
- [67] T. D. Plant, N. B. Standen, and T. A. Ward, "The effects of injection of calcium ions and calcium chelators on calcium channel inactivation in Helix neurones," *The Journal of Physiology*, vol. 334, pp. 189–212, 1983.
- [68] S. N. Gummadi, B. Bhavya, and N. Ashok, "Physiology, biochemistry and possible applications of microbial caffeine degradation," *Applied Microbiology and Biotechnology*, vol. 93, no. 2, pp. 545–554, 2012.



## Bibliography

- [69] D. A. Pelligrino, H. L. Xu, and F. Vetri, "Caffeine and the control of cerebral hemodynamics," *Journal of Alzheimer's Disease: JAD*, vol. 20, pp. 51–62, 2010.
- [70] H. Yoshimura, "The potential of caffeine for functional modification from cortical synapses to neuron networks in the brain," *Current Neuropharmacology*, vol. 3, no. 4, pp. 309–316, 2005.
- [71] E. R. O'Connor and H. K. Kimelberg, "Role of calcium in astrocyte volume regulation and in the release of ions and amino acids," *The Journal of Neuroscience*, vol. 13, no. 6, pp. 2638–2650, 1993.
- [72] T. A. Fiacco and K. D. McCarthy, "Astrocyte calcium elevations: properties, propagation, and effects on brain signaling," *Glia*, vol. 54, no. 7, pp. 676–690, 2006.
- [73] L. Welberg, "Glia: noradrenaline arouses astrocytes," *Nature Reviews Neuroscience*, vol. 15, no. 8, pp. 494, 2014.
- [74] M. Paukert, A. Agarwal, J. Cha, V. A. Doze, J. U. Kang, and D. E. Bergles, "Norepinephrine controls astroglial responsiveness to local circuit activity," *Neuron*, vol. 82, no. 6, pp. 1263–1270, 2014.
- [75] C. Chen, Z. Jiang, X. Fu, D. Yu, H. Huang, and J. G. Tasker, "Astrocytes amplify neuronal dendritic volume transmission stimulated by norepinephrine," *Cell Reports*, vol. 29, no. 13, pp. 4349–4361.e4, 2019.
- [76] K. B. Lefton, Y. Wu, A. Yen, T. Okuda, Y. Zhang, Y. Dai, S. Walsh, R. Manno, J. D. Dougherty, V. K. Samineni, P. C. Simpson, and T. Papouin, "Norepinephrine signals through astrocytes to modulate synapses," *bioRxiv: the preprint server for biology*, 2024
- [77] A. Jennings and D. A. Rusakov, "Do astrocytes respond to dopamine?" *Opera Medica et Physiologica*, vol. 2, no. 1, pp. 34–43, 2016.
- [78] A. Vaarmann, S. Gandhi, and A. Y. Abramov, "Dopamine induces Ca<sup>2+</sup> signaling in astrocytes through reactive oxygen species generated by monoamine oxidase," *Journal of Biological Chemistry*, vol. 285, no. 32, pp. 25018–25023, 2010.
- [79] M. Matias, J. Morgado, and F. C. A. Gomes, "Astrocyte heterogeneity: Impact to brain aging and disease," *Frontiers in Aging Neuroscience*, vol. 11, 2019.
- [80] S. Kanumilli and P. J. Roberts, "Mechanisms of glutamate receptor induced proliferation of astrocytes," *Neuroreport*, vol. 17, no. 18, pp. 1877–1881, 2006.
- [81] U. Sonnewald and A. Schousboe, "Introduction to the glutamate-glutamine cycle," *Advances in Neurobiology*, vol. 13, pp. 1–7, 2016.

## Bibliography

- [82] B. Hassel and R. Dingledine, "Glutamate and glutamate receptors," *Basic Neurochemistry*, pp. 342–366, 2012.
- [83] D. B. Hansen, N. Garrido-Comas, M. Salter, and R. Fern, " $\text{HCO}_3^-$ -independent pH regulation in astrocytes in situ is dominated by V-ATPase," *Journal of Biological Chemistry*, vol. 290, no. 13, pp. 8039–8047, 2015.
- [84] T. H. Oh, G. J. Markelonis, J. R. Von Visger, B. Baik, and M. T. Shipley, "Acidic pH rapidly increases immunoreactivity of glial fibrillary acidic protein in cultured astrocytes," *Glia*, vol. 13, no. 4, pp. 319–322, 1995.
- [85] M. O. Bevensee and W. F. Boron, "Control of intracellular pH," *Seldin and Giebisch's The Kidney*, pp. 1773–1835, 2013
- [86] S. M. Theparambil, G. Begum, and C. R. Rose, "pH regulating mechanisms of astrocytes: A critical component in physiology and disease of the brain," *Cell Calcium*, 2024.